

1 **Future response of global coastal wetlands to sea level rise**

2 **Mark Schuerch^{1,2*}, Tom Spencer², Stijn Temmerman³, Matthew L. Kirwan⁴, Claudia Wolff⁵, Daniel**
3 **Lincke⁶, Chris J. McOwen⁷, Mark D. Pickering⁸, Ruth Reef⁹, Athanasios T. Vafeidis⁵, Jochen**
4 **Hinkel^{6,10}, Robert J. Nicholls¹¹, Sally Brown¹¹**

5 ¹ Lincoln Centre for Water and Planetary Health, School of Geography, University of Lincoln, Lincoln,
6 United Kingdom

7 ² Cambridge Coastal Research Unit, Department of Geography, University of Cambridge, Cambridge
8 United Kingdom

9 ³ Ecosystem Management Research Group, University of Antwerp, Antwerp, Belgium

10 ⁴ Virginia Institute of Marine Science, College of William and Mary, Gloucester Point, Virginia, USA

11 ⁵ Institute of Geography, Christian-Albrechts University of Kiel, Kiel, Germany

12 ⁶ Global Climate Forum, Berlin, Germany

13 ⁷ UN Environment World Conservation Monitoring Centre, Cambridge, United Kingdom

14 ⁸ Ocean and Earth Science, National Oceanography Centre, University of Southampton,
15 Southampton, United Kingdom

16 ⁹ School of Earth, Atmosphere and Environment, Monash University, Clayton, Victoria, Australia

17 ¹⁰ Division of Resource Economics, Thae-Institute and Berlin Workshop in Institutional Analysis of
18 Social-Ecological Systems (WINS), Humboldt-University, Berlin, Germany

19 ¹¹ Faculty of Engineering and the Environment, University of Southampton, Southampton, United
20 Kingdom

21 *Corresponding author: mschuerch@lincoln.ac.uk

22

23 **Introduction**

24 **The response of coastal wetlands to sea level rise (SLR) during the 21st century remains uncertain.**
25 **Global-scale projections suggest that between 20% and 90% (for low and high SLR scenarios,**
26 **respectively) of the present-day coastal wetland area will be lost, including the loss of biodiversity**
27 **and highly valued ecosystem services¹⁻³. These projections do not necessarily take into account all**
28 **essential geomorphological⁴⁻⁷ and socio-economic system feedbacks⁸. Here we present an**
29 **integrated global modelling approach that considers (i) the ability of coastal wetlands to build up**
30 **vertically by sediment accretion and (ii) the accommodation space, namely the vertical and lateral**
31 **space available for fine sediments to accumulate and to be colonised by wetland vegetation. We**
32 **use this approach to assess global-scale changes in coastal wetland area in response to global SLR**
33 **and anthropogenic coastal occupation during the 21st century. Based on our simulations we find**
34 **that, globally, wetland gains of up to 60% of the current area are expected, if more than 37% of**
35 **coastal wetlands have sufficient accommodation space, and sediment supply remains at present**
36 **levels. In contrast to previous studies¹⁻³, we project that until 2100 global coastal wetland loss will**
37 **range between 0% and 30%, assuming no additional accommodation space. Our simulations**
38 **suggest that global wetland resilience is primarily driven by the availability of accommodation**
39 **space, which is strongly influenced by the building of anthropogenic infrastructure in the coastal**
40 **zone and its expected to change over the 21st century. Rather than being an inevitable**
41 **consequence of global SLR, our findings indicate that large-scale coastal wetland loss might be**
42 **avoidable, if sufficient additional accommodation space can be created through innovative**
43 **“nature-based adaptation” solutions to coastal management.**

44

45 **Main text**

46 Coastal wetlands provide many important ecosystem services (valued up to 194,000 USD ha⁻¹ yr⁻¹)⁹,
47 including carbon sequestration¹⁰⁻¹¹, natural coastal protection¹²⁻¹⁵, support of fisheries¹⁶ and water
48 quality improvement¹⁷. Recent global-scale assessments of coastal wetland dynamics have
49 suggested that the ability of many marshes and mangroves to build up vertically has already been
50 overwhelmed by present-day SLR, leading to widespread wetland loss¹⁻³. At the same time, more
51 regional to local-scale field measurements and models of salt marsh accretion have concluded that
52 most large-scale assessments have overestimated the vulnerability of coastal wetlands to SLR⁴.
53 These differences highlight a major knowledge gap in our understanding of coastal wetland
54 responses to global environmental change. It has been argued that the reason for the observed
55 discrepancy is that large-scale assessments have so far failed to consider the well-understood bio-
56 physical feedback mechanisms which are typically included in local-scale models⁴. These
57 mechanisms include the ability of coastal wetlands to build up vertically by sediment accretion which
58 is enhanced with increasing inundation heights and frequencies, triggered for example by
59 accelerating SLR, and which enables coastal wetlands to persist or even prosper with SLR⁵⁻⁷.

60 A second limitation of previous global-scale assessments is that they have not yet represented
61 accommodation space (the vertical and lateral space available for fine sediments to accumulate and
62 be colonised by wetland vegetation) in a spatially explicit manner^{2,4}. This constitutes an important
63 gap as recent papers have suggested that anthropogenic barriers to inland wetland migration
64 (coastal flood protection structures, coastal roads and railway lines, settlements, and impervious
65 land surfaces) may be a more important threat to coastal wetlands than drowning by SLR alone^{2,4,18}.

66 We address both of these limitations, and assess global-scale changes in coastal wetland area in
67 response to global SLR and anthropogenic coastal occupation, using a novel integrated modelling
68 approach. For the first time, we consider (1) the vertical adaptability of coastal wetlands by bio-
69 physical feedbacks between wetland accretion and SLR, assuming current-day levels of sediment

70 availability, and (2) their horizontal adaptability, as determined by the interactions between inland
71 wetland migration and anthropogenic barriers, assuming wetland inland migration to be a function
72 of accommodation space⁸. We present a model to make projections of the global resilience of
73 coastal wetlands to 21st century SLR scenarios under existing and increased accommodation space,
74 representing present conditions and two additional coastal management scenarios following the
75 wider implementation of nature-based adaptation strategies¹². By means of a comprehensive
76 sensitivity analysis, we finally assess the extent to which this resilience is controlled by vertical and
77 horizontal adaptation mechanisms.

78 Based on the simulation runs during model calibration, our calibrated model, which includes
79 mangroves, salt and freshwater tidal marshes, correctly predicts observations of present-day vertical
80 wetland change, obtained from large meta-datasets from all over the world^{3,4,19}, for 78% of all
81 coastal areas where data is currently available (N=46) (ED Table1, ED Fig.1). While performing very
82 well in regions where coastal wetlands were reported to be stable (i.e. with vertical wetland growth
83 in balance with local SLR) or drowning (i.e. slower vertical wetland growth than local SLR), our model
84 tends to underestimate the number of locations with an elevation surplus (i.e. faster vertical
85 wetland growth than local SLR). Hence our predictions of the ability of wetlands to vertically grow in
86 pace with 21st century SLR rates may be considered conservative.

87 Projections of the future extent of coastal wetlands by 2100 are based on simulations using three
88 different regionalized relative SLR scenarios (RCPs 2.6, 4.5 and 8.5 corresponding to a SLR of 29, 50
89 and 110 cm by 2100) and three human adaptation scenarios with varying degrees of available
90 accommodation space (ED Table2): i) business-as-usual (BAU) scenario in which we assume that no
91 accommodation space is available where local population densities in the 1-in-100 year coastal
92 floodplain exceed thresholds between 5 and 20 people km⁻²; ii) moderate level of nature-based
93 adaptation (NB 1) in which the population density threshold ranges between 20 and 150 people km⁻²
94 and iii) high level of nature-based adaptation (NB 2) with population density thresholds between 150

95 and 300 people km⁻². Changes in population growth during the simulation period are considered by
96 applying a scenario of national population growth rates based on the shared socio-economic
97 pathway SSP2 (IIASA)²⁰, which is characterized by a moderate, and after 2070 slowing, global
98 population growth leading to 9 billion people by 2100²¹.

99 Under all SLR scenarios, 20 people km⁻² constitutes a critical population density threshold. If a higher
100 population density threshold is applied, more coastal wetlands have sufficient accommodation
101 space to migrate inland resulting in an overall gain in global coastal wetland area (Fig. 1). If lower
102 thresholds are considered, less coastal wetlands have sufficient accommodation space resulting in
103 an overall global loss. The population density threshold of 20 people km⁻² corresponds to what we
104 estimate as the current global average above which coastal communities are protected by some kind
105 of coastal protection infrastructure (Supplementary Information), hence allowing inland migration
106 for only 37% of all global coastal wetlands. A population density threshold of 300 people km⁻² is the
107 lower threshold for urban developments, as defined by the European Commission²², and sets the
108 upper limit for potential wetland inland migration (NB 2 scenario). The highest SLR scenario at this
109 threshold results in a substantial increase in global coastal wetland area (+60%). The same SLR
110 scenario with a threshold population density of 5 people km⁻² results in a net global loss of 30% (Fig.
111 1). When applying the lowest SLR scenario, areal coastal wetland changes for population density
112 thresholds between 5 and 300 people km⁻² only range between -8% (loss) and +15% (gain) (Fig. 1).
113 The largest changes are observed for mangroves, which make the largest contribution to the global
114 wetland area from the beginning (69%). Interestingly, hardly any losses are observed for salt
115 marshes, even under the human adaptation scenarios with the least accommodation space (Fig. 1).

116 Under the business-as-usual (BAU) scenario for accommodation space (5-20 people km⁻²), changes in
117 the extent of global coastal wetlands range between -8% (loss) and 0% (no change) for the lowest
118 SLR scenario and between -30% (loss) and -8% (loss) for the highest SLR scenario. These losses can
119 primarily be attributed to an increasing sediment deficiency, impeding the wetland's ability to

120 vertically keep pace with SLR. If, in the future, coastal wetlands are given more accommodation
121 space (e.g. in the context of the implementation of nature-based adaptation solutions), global
122 coastal wetlands could increase in areal extent (Fig. 1). Our moderate nature-based adaptation
123 scenario (NB 1: 20-150 people km⁻²) results in an increase between 0% and 12% for the low, and
124 between -8% (loss) and 42% for the high, SLR scenario. Under the more extreme adaptation scenario
125 (NB 2: 150-300 people km⁻²) we anticipate even higher increases, between 12% and 15% for the low,
126 and between 42% and 60% for the high, SLR scenario (Fig. 1). In contrast to the BAU scenario, these
127 gains for the moderate and extreme nature-based adaptation scenarios (NB 1 and NB 2) are driven
128 by inland wetland migration rather than vertical sediment accretion, therefore independent of
129 sediment availability.

130 Under the BAU scenario (lower boundary: 5 people km⁻²), the majority of the absolute loss in coastal
131 wetland areas (ca. 66%) is projected to occur in the Caribbean Sea, the southern US east coast and
132 parts of south-east Asia (Fig. 2a). Similarly, Lovelock et al.¹⁹ identified south-east Asia as a highly
133 critical region for mangrove resilience to SLR. The patterns of expected relative changes in wetland
134 areas (i.e. percent gain or loss) are somewhat different but essentially confirm the model results of
135 Spencer et al.²; largest relative area losses (again, under a scenario of highly constrained
136 accommodation space) are found in the Caribbean Sea, along the eastern US coast as well as in the
137 western Baltic Sea, the Mediterranean Sea, the Red Sea and in parts of south-east Asia (Fig. 2b).

138 The spatial patterns of coastal wetland loss strongly resemble those of the modelled present-day
139 sediment balance, namely the difference between the sediment required for a coastal wetland
140 surface to keep pace vertically with current local relative SLR and the current-day sediment
141 availability (Fig. 3). For example, large regions of sediment deficit are identified in the Caribbean Sea,
142 western Baltic Sea, Mediterranean Sea, and along the US east and west coasts (Fig. 3). These areas
143 largely coincide with the hotspot regions for relative wetland area losses under a scenario of highly
144 constrained accommodation space (Fig. 2). Meanwhile, most parts of Asia, South America and

145 North-West Europe show sufficient or excess sediment availability (Fig. 3) which correspond to areas
146 with small relative wetland loss, even where accommodation space is limited, as vertical sediment
147 accretion counteracts relative SLR (Fig. 2a).

148 Our sensitivity analysis confirms the importance of accounting for vertical sediment accretion with
149 our “sediment accretion only” scenario (scenario HYS 2, ED Table2). This scenario reduces the global
150 loss of coastal wetlands from 38% to 20%, 50% to 26% and 77% to 54% for the low, medium and
151 high SLR scenarios respectively, as compared to our “no resilience” scenario where no
152 accommodation space and no vertical sediment accretion is assumed (scenario HYS 4, ED Table2, ED
153 Fig.2).

154 Previous studies have highlighted the dangers of low sediment availability and reduced sediment
155 supply, threats that may be exacerbated regionally by increasing numbers of dams being built within
156 river catchments, causing increased risk for coastal wetland loss with SLR²⁴⁻²⁶. However, our model
157 sensitivity analysis under the high SLR scenario (RCP 8.5), and accounting for vertical sediment
158 accretion, demonstrates that if present-day values of sediment supply were to change by +/-50%,
159 only a ±6% change in global wetland area would result (ED Table3). In contrast, accommodation
160 space for inland wetland migration has a much stronger control on wetland persistence with SLR, yet
161 much less is known about the actual process and further research is urgently needed. Our sensitivity
162 analysis shows that even in heavily sediment-starved regions, an increase in accommodation space
163 could result in a net wetland gain (ED Fig.3), particularly under high rates of SLR, even though the
164 wetland’s seaward side could regularly be lost due to the lack of sediment. Under extreme rates of
165 SLR, and where sediment availability is insufficient, future coastal wetlands may therefore have a
166 shorter lifetime and a lower degree of geomorphological, hydrological and biogeochemical
167 complexity²⁷.

168 It should be noted that locally and especially in delta regions, these global mechanisms may not be
169 as straight forward because historical and contemporary catchment and delta practices (e.g. river

170 damming and dredging) are responsible for much of the observed coastal wetland trends in many
171 “loss hotspots” rather than global SLR²⁶. Also, constraints on the inland migration of coastal
172 wetlands may arise from adverse soil conditions, particularly where the inundated land has been
173 intensively modified by humans, unsuitable geomorphological characteristics or elevation
174 constraints (if located too low in the tidal frame)^{27,28}. In order to alleviate these constraints, coastal
175 management strategies and engineering may locally be required to facilitate coastal wetlands to
176 migrate inland²⁷. As a consequence, local patterns of wetland resilience may be at considerable
177 variance with global estimates of change.

178 Our model projections suggest that nature-based adaptation solutions that maximise the inland
179 migration of tidal wetlands in response to SRL, wherever possible, may help safeguard wetland
180 persistence with SLR and protect associated ecosystem services. Existing nature-based adaptation
181 solutions that allow coastal wetlands to migrate inland include the inland displacement of coastal
182 flood defences (typically along highly engineered coastlines)¹² or the designation of nature reserve
183 buffers in upland areas surrounding coastal wetlands¹⁸. These schemes, however, are currently
184 implemented as local-scale projects only; strategically upscaling such projects, such as for example
185 suggested by the so-called shoreline management plans in England and Wales²⁹ or the Coastal
186 Master Plan in Louisiana³⁰ may help coastal wetlands adapt to SLR at the landscape scale and protect
187 rapidly increasing global coastal populations.

188 **References**

- 189 1 Blankespoor, B., Dasgupta, S. & Laplante, B. Sea-Level Rise and Coastal Wetlands. *Ambio* **43**,
190 996-1005 (2014).
- 191 2 Spencer, T. *et al.* Global coastal wetland change under sea-level rise and related stresses:
192 The DIVA Wetland Change Model. *Global and Planetary Change* **139**, 15-30 (2016).
- 193 3 Crosby, S. C. *et al.* Salt marsh persistence is threatened by predicted sea-level rise. *Estuarine,*
194 *Coastal and Shelf Science* **181**, 93-99 (2016).
- 195 4 Kirwan, M. L., Temmerman, S., Skeehan, E. E., Guntenspergen, G. R. & Fagherazzi, S.
196 Overestimation of marsh vulnerability to sea level rise. *Nature Climate Change* **6**, 253-260
197 (2016).
- 198 5 Schuerch, M., Vafeidis, A., Slawig, T. & Temmerman, S. Modeling the influence of changing
199 storm patterns on the ability of a salt marsh to keep pace with sea level rise. *Journal of*
200 *Geophysical Research: Earth Surface* **118**, 84-96 (2013).

201 6 French, J. R. Numerical simulation of vertical marsh growth and adjustment to accelerated
202 sea-level rise, North Norfolk, U.K. *Earth Surface Processes and Landforms* **18**, 63-81 (1993).

203 7 Morris, J. T., Sundareshwar, P. V., Nietch, C. T., Kjerfve, B. & Cahoon, D. R. Responses of
204 coastal wetlands to rising sea level. *Ecology* **83**, 2869-2877 (2002).

205 8 Enwright, N. M., Griffith, K. T. & Osland, M. J. Barriers to and opportunities for landward
206 migration of coastal wetlands with sea-level rise. *Frontiers in Ecology and the Environment*
207 **14**, 307-316 (2016).

208 9 Costanza, R. *et al.* Changes in the global value of ecosystem services. *Global Environmental*
209 *Change* **26**, 152-158 (2014).

210 10 Duarte, C. M., Losada, I. J., Hendriks, I. E., Mazarrasa, I. & Marba, N. The role of coastal plant
211 communities for climate change mitigation and adaptation. *Nature Climate Change* **3**, 961-
212 968 (2013).

213 11 McLeod, E. *et al.* A blueprint for blue carbon: toward an improved understanding of the role
214 of vegetated coastal habitats in sequestering CO₂. *Frontiers in Ecology and the Environment*
215 **9**, 552-560 (2011).

216 12 Temmerman, S. *et al.* Ecosystem-based coastal defence in the face of global change. *Nature*
217 **504**, 79-83 (2013).

218 13 Möller, I. *et al.* Wave attenuation over coastal salt marshes under storm surge conditions.
219 *Nature Geoscience* **7**, 727-731 (2014).

220 14 Shepard, C. C., Crain, C. M. & Beck, M. W. The protective role of coastal marshes: a
221 systematic review and meta-analysis. *PLOS ONE* **6**, e27374 (2011).

222 15 Stark, J., Van Oyen, T., Meire, P. & Temmerman, S. Observations of tidal and storm surge
223 attenuation in a large tidal marsh. *Limnology and Oceanography* **60**, 1371-1381 (2015).

224 16 Aburto-Oropeza, O. *et al.* Mangroves in the Gulf of California increase fishery yields.
225 *Proceedings of the National Academy of Sciences* **105**, 10456-10459 (2008).

226 17 Teuchies, J. *et al.* Estuaries as filters: the role of tidal marshes in trace metal removal. *PLOS*
227 *ONE* **8**, e70381 (2013).

228 18 Kirwan, M. L. & Megonigal, J. P. Tidal wetland stability in the face of human impacts and sea-
229 level rise. *Nature* **504**, 53-60 (2013).

230 19 Lovelock, C. E. *et al.* The vulnerability of Indo-Pacific mangrove forests to sea level rise.
231 *Nature* **526**, 559-563 (2015).

232 20 van Vuuren, D. P. *et al.* A new scenario framework for climate change research: scenario
233 matrix architecture. *Climatic Change* **122**, 373-386 (2014).

234 21 KC, S. & Lutz, W. The human core of the shared socioeconomic pathways: Population
235 scenarios by age, sex and level of education for all countries to 2100. *Global Environmental*
236 *Change* **42**, 181-192 (2017).

237 22 Dijkstra, L. & Poelman, H. *A harmonised definition of cities and rural areas: the new degree*
238 *of urbanisation*. (European Commission, 2014).

239 23 Day, J. W., Pont, D., Hensel, P. F. & Ibàñez, C. Impacts of sea-level rise on deltas in the Gulf of
240 Mexico and the Mediterranean: The importance of pulsing events to sustainability. *Estuaries*
241 **18**, 636-647 (1995).

242 24 Yang, S. L. *et al.* Impact of dams on Yangtze River sediment supply to the sea and delta
243 intertidal wetland response. *Journal of Geophysical Research: Earth Surface* **110**, F03006
244 (2005).

245 25 Ganju, N. K. *et al.* Spatially integrative metrics reveal hidden vulnerability of microtidal salt
246 marshes. *Nature Communications* **8**, 14156 (2017).

247 26 Jankowski, K. Törnqvist, T. E. & Fernandes, A. M. Vulnerability of Louisiana's coastal wetlands
248 to present-day rates of relative sealevel rise, *Nature Communications* **8**, 14792. (2017).

249 27 Spencer, K. L. *et al.* Physicochemical changes in sediments at Orplands Farm, Essex, UK
250 following 8 years of managed realignment. *Estuarine, Coastal and Shelf Science* **76**, 608-619
251 (2008).

- 252 28 French, P. W. Managed realignment - The developing story of a comparatively new approach
253 to soft engineering. *Estuarine, Coastal and Shelf Science* **67**, 409-423 (2006).
- 254 29 Nicholls, R. J., Townend, I. H., Bradbury, A. P., Ramsbottom, D. & Day, S. A. Planning for long-
255 term coastal change: Experiences from England and Wales. *Ocean Engineering* **71**, 3-16
256 (2013).
- 257 30 Peyronnin, N. *et al.* Louisiana's 2012 Coastal Master Plan: Overview of a Science-Based and
258 Publicly Informed Decision-Making Process. *Journal of Coastal Research* **S167**, 1-15 (2013).

259 **Acknowledgement**

260 This research was financially supported by the 'Deutsche Forschungsgemeinschaft' (DFG) through
261 the Cluster of Excellence 80 'The Future Ocean', funded within the framework of the Excellence
262 Initiative on behalf of the German federal and state governments, the personal research fellowship
263 of Mark Schuerch (Project Number 272052902) and by the Cambridge Coastal Research Unit (Visiting
264 Scholar Programme). Furthermore, this work has partly been supported by the EU research project
265 RISES-AM- (FP7-ENV-693396).

266 We thank M. Martin for support in editing the calibration data and G. Amable for valuable statistical
267 advice.

268 **Author contributions**

269 M.S., T.S. developed the model algorithm. M.S., D.L. developed the model code. M.S., C.W., C.McO.,
270 M.D.P., M.L.K., A.T.V., R.R., S.B. gathered/produced input data. M.S., S.T., R.J.N. analysed /
271 interpreted the model simulations. M.S., T.S., S.T. M.L.K., J.H. wrote the paper.

272 **Author information**

273 The authors declare no competing interests.

274 **Figure legends**

275 Figure 1: Global change (km²) in coastal wetland areas. Results are displayed for all three SLR
276 scenarios (RCP 2.6 - low, RCP 4.5 - medium, RCP 8.5 - high) and three human adaptation scenarios,
277 defined by different population density thresholds (BAU 1: 5 - 20 people km⁻², NB 1: 20 - 150 people
278 km⁻², NB 2: 150 - 300 people km⁻²). Sediment accretion is considered, and wetland inland migration

279 is limited to where the population density in the 1-in-100 year floodplain falls below the respective
280 threshold. Areal changes of all three wetland types are indicated in the tables below the graphs.

281 Figure 2: Spatial distribution of coastal wetland change. Absolute (a) and relative (b) changes in
282 coastal wetland areas are displayed for the medium SLR scenario (RCP4.5 (med)), assuming
283 inhibition of wetland inland migration everywhere, but in (nearly) uninhabited regions with a
284 population density <5 people km^{-2} . Population density is subject the population growth throughout
285 the simulation period, following the shared socio-economic pathway SSP2^{21,22}. The displayed
286 coastline was generated during the DINAS-COAST FP5-EESD EU project (EVK2-CT-2000-00084).

287 Figure 3: Present-day global sediment balance. Sediment surplus (positive values) or sediment
288 deficits (negative values) (in mg l^{-1}) represent the difference between the sediment concentration
289 needed for coastal wetlands to vertically build up with current SLR rates and the actual sediment
290 concentration derived from the satellite-borne Globcolour data (<http://globcolour.info>). The
291 displayed coastline was generated during the DINAS-COAST FP5-EESD EU project (EVK2-CT-2000-
292 00084).

293 **Methods**

294 *General description of Model approach*

295 Our model is based on the construction of coastal profiles for 12,148 coastline segments. These
296 segments constitute the spatial units of the *Dynamic Interactive Vulnerability Assessment (DIVA)*
297 modelling framework^{31,32}. The coastal profiles are derived from the Shuttle Radar Topography
298 Mission (SRTM) floodplain data, available from the global DIVA database³³. Within each coastline
299 segment, the existing coastal wetlands, as reported by the United Nations Environment Programme
300 World Conservation Monitoring Centre (UNEP WCMC)^{34,35}, are assumed to be located between
301 mean sea level (MSL) and mean high water spring (MHWS) level. With SLR, the seaward side of the
302 wetlands are increasingly inundated (“unconstrained wetland loss”), while the landward side
303 migrates inland by converting terrestrial uplands to coastal wetlands (Figs. ED1, ED2)³⁶. However,
304 inland wetland migration may be inhibited by anthropogenic coastal infrastructure reducing the
305 available accommodation space³⁶⁻³⁹, a variable that we approximate with the population density in
306 the floodplain of the 1-in-100 year extreme water level (ED Fig.4).

307 Seaward wetland loss through inundation is counteracted by a large tidal range and a high sediment
308 availability, as both these variables increase the resilience of coastal wetlands towards drowning
309 through vertical sediment accretion processes^{19,40-44}. This is represented by the Wetland Adaptability
310 Score (WAS) reducing the loss of wetlands where tidal range and sediment availability are high⁴⁰ (ED
311 Fig.4). The calculation of the WAS is based on a linear relationship between sediment availability and
312 wetland drowning, whereas the slope of the linear relationship depends on tidal range. This
313 relationship was suggested by Kirwan et al.⁴⁰, who ran an ensemble of five different tidal marsh
314 accretion models to identify the critical rates of relative SLR as a function of tidal range and sediment
315 availability.

316 Following the calculation of the seaward wetland loss and inland wetland gain, the resulting global
317 coastal wetland areas are calculated for every model time step (5 years) between 2010 and 2100.

318 The model is driven by temporal changes in the model variables “Regional relative sea level rise” and
319 “Population density” according to a range of regionalized scenarios for global SLR (Representative
320 Concentration Pathways: RCPs)⁴⁵ and the shared socio-economic pathway SSP2²⁰ for national
321 population growth respectively (ED Table2, ED Fig.4).

322 *Input data*

323 Database and data model

324 The input variables are derived from spatially explicit global datasets. They are attributed to the
325 12,148 coastline segments, which have an average length of 57 km³¹. Coastline segmentation is a
326 product of the DIVA modelling framework; the related database includes more than 100 bio-physical
327 and socio-economic parameters³¹. The dissection of the global coastline into segments is based on
328 the concept of McFadden et al.⁴⁶, where coastal units have been created such that bio-physical and
329 socio-economic impacts of global SLR are expected to be comparable within each coastline segment.

330 Construction of the coastal topographic profile

331 For each of the DIVA coastline segments, the coastal topographical profile is approximated using the
332 areal information on coastal floodplains taken from Hinkel et al.³². They provide floodplain areas
333 (km²) for the elevation increments <1.5 m, 1.5-2.5 m, 2.5-3.5 m, 3.5-4.5 m, 4.5-5.5 m, 5.5-8.5 m, 8.5-
334 12.5 m, 12.5-16.5 m, based on freely available Shuttle Radar Terrain Mission (SRTM) data⁴⁷. The
335 SRTM data has a 90 m horizontal and a 1 m vertical resolution. The coastal profiles are constructed
336 by dividing the floodplain areas per elevation increment by the length of the corresponding coastline
337 segment in order to calculate the inundation lengths, which are then plotted against the upper
338 boundaries of the elevation increments (i.e. 1.5 m, 2.5 m, 3.5 m, etc.) (ED Fig.5). It is thereby
339 assumed that elevations continuously increase with distance from the coast, which has been shown
340 to be a reasonable assumption³³.

341 Elevations between the upper boundaries of the elevation increments are linearly interpolated
342 following earlier global assessments^{32,48-50}. Titus and Richman⁵¹ and Titus and Wang⁵² who linearly
343 interpolated between the MHWS level and an elevation of 1.5 m (or higher) showed that their
344 method approximated high resolution LIDAR-derived elevations with a mean error of less than 30 cm
345 and that linear interpolation produces no systematic bias with respect to the area of inundated land,
346 even for the lowest 50 cm of the profile⁵².

347 Wetland data

348 The areal wetland extents utilized in the context of this study include current wetland areas (1973-
349 2015) for 'Mangrove forests'³⁴, 'Salt marshes'³⁵ and 'Tidal freshwater marshes'⁵³. Based on a
350 literature search for the lower and upper elevation limits of mangroves, salt marshes and tidal
351 freshwater marshes⁵³⁻⁵⁷, we assume that all coastal wetland types are located at elevations between
352 MSL and MHWS and can occur over the entire elevation range. The reported wetland areas for each
353 coastline segment are distributed alongside the non-wetland floodplain on the previously
354 constructed coastal profile (ED Fig.5). We appreciate that in nature, the upper and lower boundaries
355 of coastal wetlands will vary as a result of different vegetation species, tidal currents and waves⁵⁹,
356 but for our global application MSL as the lower, and MHWS as the upper, limit constitute solid
357 boundaries.

358 Regional relative sea level rise data and scenarios

359 We use three SLR scenarios, covering the range of global SLR as projected by the IPCC AR5⁴⁵ plus a
360 possible greater contribution of ice-sheets as assessed on the basis of post-AR5 methods³². The
361 three scenarios represent the three representative concentration pathways (RCPs) 2.6, 4.5, and 8.5,
362 paired with a low, medium and high ice-sheet contribution respectively, and generated using the
363 general circulation model HadGEM2-ES⁶⁰ (ED Table2). The employed SLR scenarios are regionalized,
364 therefore accounting for regional gravitational and rotational effects due to changes in ice mass

365 distribution and steric variation³². Local relative SLR information is attained by combining the
366 regionalized SLR projections with segment-specific vertical land movement based on a global model
367 of glacial isostatic adjustment (GIA)⁶¹ and some additional 2 mm yr⁻¹ of natural subsidence in large
368 river deltas^{62,63} (ED Fig.6). Meanwhile, human-induced subsidence, which may be of particular
369 importance in large river deltas⁶⁴, is not considered for calculating regional relative SLR. However, a
370 sensitivity analysis using a delta-wide subsidence rates of 5 mm yr⁻¹ showed only small deviation in
371 overall global wetland areas (ED Table4). Tectonic and neotectonic uplift/subsidence processes,
372 other than GIA, are also not included due to the lack of an appropriate global dataset.

373 Tidal range data

374 In order to calculate the WAS (ED Fig.4) and compute the vertical wetland extent within each
375 coastline segment, we use a newly developed global tidal range dataset⁶⁵, representing the
376 segment-specific mean low water (MLW), mean high water (MHW), mean high water neap (MHWN)
377 and mean high water spring (MHWS) tidal levels. The new tidal dataset was generated using
378 OTISmpi⁶⁶, a forward global tidal model, solving the non-linear shallow water equations on a C-grid
379 using a finite differences time stepping method (Supplementary Information).

380 Population density

381 For each coastline segment, the coastal population within each elevation increment is computed by
382 superimposing the SRTM digital elevation model⁴⁷ with the Global Rural-Urban Mapping Project
383 (GRUMP) population data⁶⁷, being subject to national population growth according to SSP2
384 (IIASA)^{20,68}. To determine the population density in the floodplain of the 1-in-100 year extreme water
385 level, which is used as a proxy for the availability of accommodation space (ED Fig.4), we derive the
386 hydrologically connected floodplain area for the 1-in-100 year extreme water level and the
387 corresponding population affected by flooding³². We use the latest dataset on extreme water levels
388 along the world's coastline, produced with a new global storm surge model hindcasting extreme

389 water levels between 1979 and 2014⁵⁰. Extreme water levels are reported for the return periods of
390 1, 10, 100 and 1000 years and are derived from total water levels during storm surge events, thus
391 including both tides and surges.

392 Sediment availability

393 Local sediment availability is derived from MERIS satellite data, processed in the framework of the
394 Globcolour project (<http://globcolour.info>). The data represent total suspended matter (TSM) in the
395 water column and have been developed, validated, and distributed by ACRI-ST, France⁶⁹. We use the
396 monthly averages from April 2002 to April 2012 that have a horizontal resolution of 1/24°. A long-
397 term average is calculated for every pixel, and an average value of all pixels located within a 4 km
398 buffer of each coastline segment is used to represent the local sediment availability (mg l⁻¹).

399 *Sea-level rise impacts on coastal wetlands*

400 Conversion of terrestrial upland to coastal wetlands

401 With increasing sea levels, we allow coastal wetlands to migrate inland, a process that we
402 understand as the establishment of wetland vegetation inland of its previous location, by raising the
403 MHWs level along the coastal profile. Hence, former terrestrial upland areas are inundated and
404 converted to coastal wetlands (ED Fig.5), based on elevation, where no human barriers are assumed
405 to be present³⁶⁻³⁹. This modelling approach is supported by recent local-scale field studies for coastal
406 salt marshes at the US east coast and in the Gulf of Mexico⁶⁹⁻⁷⁴ and has previously been applied
407 through various local-scale models, both for salt marshes and mangroves⁷⁵⁻⁷⁹. The establishment of
408 coastal wetland vegetation in inundated upland areas is assumed to be associated with a response
409 lag of five years, which is in line with evidence produced by recent wetland restoration studies⁸⁰⁻⁸³.
410 However, the development of related wetland functions (such as biogeochemical functioning) may
411 take more time^{74,80}.

412 For calculation of the converted upland areas, we assume the segment-specific wetland/non-
413 wetland proportion to remain constant over time, whereby the non-wetland area within a coastline
414 segment equals the total floodplain area (i.e. the total interpolated area between MSL and MHWS)
415 minus the reported wetland area. The conversion of uplands to wetlands is therefore calculated as
416 the product of the wetland/non-wetland proportion and the total inundated upland area. However,
417 conversion of terrestrial upland to coastal wetland is assumed to be zero where the coastal
418 population density within the floodplain of the 1-in-100 year extreme water level exceeds the given
419 thresholds (5, 20, 150 or 300 people km⁻²), representing the existence of anthropogenic barriers to
420 inland wetland migration. We thereby assume that coastal protection infrastructure is an important
421 contributor to anthropogenic barriers for wetland inland migration^{2,8,36-39} and is built where coastal
422 communities are threatened by extreme water levels, such as a 1-in-100 year event^{32,84}.

423 Seaward loss of coastal wetlands

424 As sea level rises, not only the upper wetland boundary (MHWS) but also the lower wetland
425 boundary (MSL) shifts position, potentially causing inundation of coastal wetlands beyond
426 physiological tolerance. Therefore, we calculate an “unconstrained seaward loss” which at first
427 neglects the wetland’s capacity to vertically adapt to SLR by sediment accretion (Fig.ED2). Through
428 sediment accretion, this unconstrained seaward loss may, however, be reduced or inhibited, given
429 sufficient sediment availability within the coastline segment (ED Fig.4).

430 The Wetland Adaptability Score (WAS) is a measure for the difference between the sediment needed
431 for the coastal wetland to vertically accrete sediment as fast as SLR and the sediment available. It
432 represents a sediment surplus if positive, and a sediment deficit if negative (Fig. 3). The amount of
433 sediment needed for a coastal wetland to adapt to SLR has been studied by Kirwan et al.⁴⁰, using an
434 ensemble of five models for tidal marsh accretion. They present linear relationships between
435 sediment availability and the maximum rate of relative SLR that a tidal marsh can survive, showing
436 steeper slopes (higher resilience) for marshes in macrotidal environments compared to marshes in

437 microtidal environments. We directly use these linear relationships for our tidal marshes (including
438 tidal salt and freshwater marshes), whereas we modify the model parameters for modelling
439 mangrove forests during our calibration procedure (Supplementary Information). The local sediment
440 availability, as derived from the Globcolour data, is assumed to represent the current levels of TSM
441 in the coastal zone and assumed to remain constant during the simulation period. To account for
442 possible changes in future global sediment supply, a sensitivity analysis has been conducted with
443 average sediment availability levels reduced and increased by 20% and 50% (ED Table3).

444 The WAS thus represents the ability of the coastal wetlands within a coastline segment to adapt to
445 rising sea levels by sediment accretion. A positive WAS implies that sediment availability is sufficient
446 to maintain the present wetland area whereas a negative WAS implies that coastal wetlands are
447 inundated and (partially) lost in response to SLR. The WAS is an integer value that ranges from -5 to
448 +5, indicating a very high (-5) to very low (-1) sediment deficiency and a very low (+1) to very high
449 (+5) sediment surplus respectively. Based on the WAS (WAS), the unconstrained seaward loss (SL_{unc} :
450 km^2) is transformed into a constrained seaward loss (SL_c : km^2), assuming a linear relationship
451 between WAS and the proportion of inundated wetland actually being lost, but only if WAS is
452 negative (eq. 1). No wetland loss is computed where WAS is positive or zero. With SLR both WAS and
453 SL_{unc} change over time. Thus SL_c is updated after every time step (t_i).

$$454 \quad SL_c(t_i) = (-1/5) * WAS(t_i) * SL_{unc}(t_i) \quad (\text{eq. 1})$$

455 The calculation of WAS is based on the assumption that the critical rate of relative SLR ($RSLR_{crit}$: mm
456 yr^{-1}) depends on sediment availability (Sed : $mg\ l^{-1}$) and tidal range (TR), as suggested by Kirwan et
457 al.⁴⁰. Their modelling results can be approximated using the following relationship (eq. 2):

$$458 \quad RSLR_{crit} = (m * TR^e) * Sed + i \quad (\text{eq. 2})$$

459 where $(m * TR^e)$ represents the slope of a linear relationship between $RSLR_{crit}$ and Sed . Model
460 parameters e , i and m are calibrated separately for tidal marshes (including tidal salt and freshwater

461 marshes, e_{TF} , i_{TF} and m_{TF}) and mangrove systems (e_{Man} , i_{Man} and m_{Man}). Parameters e_{TF} , i_{TF} and m_{TF} are
462 directly derived from the model ensemble runs of Kirwan et al.⁴⁰ and e_{Man} , i_{Man} and m_{Man} are
463 estimated by calibrating the model using the mangrove data presented by Lovelock et al.¹
464 (Supplementary Information).

465 To estimate the sediment needed for a given SLR rate, Sed_{crit} ($mg\ l^{-1}$), we rewrite equation 2 as
466 follows (eq. 3):

$$467 \quad Sed_{crit} = (RSLR - i) / (m * TR^a) \quad (\text{eq. 3})$$

468 where $RSLR$ ($mm\ yr^{-1}$) is the actual (time dependent) local relative SLR rate. Knowing the current
469 sediment availability (Sed) within each coastline segment (derived from the Globcolour data), we
470 compare this value with the segment-specific Sed_{crit} and define WAS as the scaled and rounded
471 difference between the available and needed sediment availability (eq. 4):

$$472 \quad WAS = \text{round}((Sed - Sed_{crit}) / a * 5) \quad (\text{eq. 4})$$

473 where a represents the sediment surplus (or deficit in case $sedsup < sedsup_{crit}$), which is considered
474 as “very high”. The determination of a is subject to model calibration (Supplementary Information).
475 All WAS values greater (smaller) than 5 (-5) are transformed to WAS values of 5 (-5).

476 *Model calibration*

477 The model parameters m_{TF} , m_{Man} , e_{TF} , e_{Man} , i_{TF} , i_{Man} and a (eqs. 3+4) are estimated using a stepwise
478 calibration procedure as described in detail in the Supplementary Information. Model results are
479 thereby compared to field measurements of vertical elevation growth for 39 marsh sites across US
480 and European Atlantic shorelines⁴, 18 marsh sites in North America, Europe and north-east
481 Australia³ and 26 mangrove sites across Pacific shorelines³. The calibrated model ($m_{TF}=3.42$,
482 $m_{Man}=4.42$, $e_{TF}=0.915$, $e_{Man}=1.18$, $i_{TF}=1.5$, $i_{Man}=0$ and $a=40\ mg\ l^{-1}$) correctly predicts whether there is a

483 sediment deficit, a sediment surplus or a balanced sediment budget for 78% of the coastline
484 segments where field data is available (ED Table1).

485 *Scenarios*

486 The three SLR scenarios RCP 2.6, 4.5 and 8.5, accounting for the full range of available SLR
487 scenarios⁴⁵, are combined with three human adaptation scenarios. These are subject to population
488 growth according to SSP 2 (ED Table2) which is considered a middle-of-the-road scenario for
489 population growth⁶⁸. The three different human adaptation scenarios include a business-as-usual
490 (BAU) scenario, a moderate nature-based adaptation scenario (NB 1) and an extreme nature-based
491 adaptation scenario (NB 2). They reflect differences in the potential of coastal wetlands to migrate
492 inland until 2100 due to potential differences in future coastal management strategies. In addition,
493 four different physically and/or socio-economically unrealistic model configurations (ED Table2:
494 hypothetical scenarios) were used during the sensitivity analysis to quantify the extent to which
495 overall resilience is enabled/constrained by vertical and horizontal adaptability mechanisms, namely
496 vertical sediment accretion and wetland inland migration.

497 Human adaptation scenarios

498 Inland/upward migration of coastal wetlands is often obstructed by the presence of anthropogenic
499 infrastructure (e.g. dikes, seawalls, cities, roads, railways, etc.)^{18,37}. As there is no global dataset on
500 coastal infrastructure, we approximate accommodation space through a population density
501 threshold above which we assume that no accommodation space is available for coastal wetlands to
502 migrate inland/upward. We thereby assume that coastal infrastructure is more likely to be present,
503 where population density is high^{37,85}, and that coastal protection structures are among the most
504 important barriers for wetland inland migration⁸. By comparing a recent expert judgement on
505 current coastal protection infrastructure, relying on population density and Gross National Income
506 (GNI)⁸⁶, with coastal population densities within the 1-in-100 year extreme water level floodplain,
507 we find that currently, on a global average, coasts of >20 people km⁻² are protected by some kind of

508 coastal protection infrastructure (Supplementary Information). We consider this number as the
509 upper boundary of current accommodation space. This is because it only includes coastal protection
510 infrastructure and neglects other anthropogenic infrastructure that may act as barrier. As a lower
511 boundary we choose a population density threshold of 5 people km⁻² as this has previously been
512 used to define (nearly) uninhabited land⁸⁷. We therefore define the range of threshold population
513 densities between 5 and 20 people km⁻² as our BAU scenario (Fig. 1 and ED Table2).

514 In two nature-based adaptation scenarios (NB 1 and NB 2) we assume that coastal societies in rural
515 areas retreat from the coast with SLR, removing coastal protection and other infrastructure that
516 inhibit inland migration of coastal wetlands. We thereby assume that this is more likely to happen in
517 sparsely populated areas as compared to densely populated areas^{8,88-90}. For the first nature-based
518 adaptation scenario (NB 1), we assume an upper boundary of 150 people km⁻² which corresponds to
519 the OECD definition of urban areas⁹¹. In the second, more extreme nature-based adaptation scenario
520 we use a threshold of 300 people km⁻² as the upper boundary, since this corresponds to the
521 European Commission's definition of urban areas²² (ED Table2).

522 Hypothetical scenarios

523 The four hypothetical scenarios used for the sensitivity analysis include: (1) "wetland migration
524 only", characterized by the exclusion of bio-physical vertical accretion mechanisms and unlimited
525 inland accommodation space; (2) "sediment accretion only", characterized by the inclusion of bio-
526 physical vertical accretion mechanisms, but assuming no inland accommodation space; (3)
527 "maximum resilience", which includes bio-physical accretion mechanisms and assumes an unlimited
528 potential for inland migration; and (4) "no resilience" where neither bio-physical accretion nor inland
529 migration are accounted for (ED Table2).

530 It should be noted that these hypothetical scenarios are unrealistic from a socio-economic and/or
531 physical perspective, since no future coast will be neither completely defended nor completely

532 undefended by dikes and seawalls and neither will sediment accretion be fully absent. But these
533 hypothetical model runs are meant to demonstrate the relative contributions of the two
534 mechanisms of wetland inland migration and sediment accretion to the overall wetland resilience to
535 SLR.

536 References

- 537 31 Vafeidis, A. T. *et al.* A new global coastal database for impact and vulnerability analysis to
538 sea-level rise. *Journal of Coastal Research* **24**, 917-924 (2008).
- 539 32 Hinkel, J. *et al.* Coastal flood damage and adaptation costs under 21st century sea-level rise.
540 *Proceedings of the National Academy of Sciences* **111**, 3292-3297 (2014).
- 541 33 Vafeidis, A. T. *et al.* Water-level attenuation in broad-scale assessments of exposure to
542 coastal flooding: a sensitivity analysis. *Natural Hazards and Earth System Sciences*
543 *Discussions*, doi:10.5194/nhess-2017-199 (2017).
- 544 34 Giri, C. *et al.* Status and distribution of mangrove forests of the world using earth
545 observation satellite data. *Global Ecology and Biogeography* **20**, 154-159 (2011).
- 546 35 McOwen, C. *et al.* A global map of saltmarshes. *Biodiversity Data Journal* **5**, e11764 (2017).
- 547 36 Kirwan, M. L., Walters, D. C., Reay, W. G. & Carr, J. A. Sea level driven marsh expansion in a
548 coupled model of marsh erosion and migration. *Geophysical Research Letters* **43**, 4366-4373
549 (2016).
- 550 37 Borchert, S. M., Osland, M. J., Enwright, N. M. & Griffith, K. T. Coastal wetland adaptation to
551 sea level rise: Quantifying potential for landward migration and coastal squeeze. *Journal of*
552 *Applied Ecology* (2018).
- 553 38 Gilman, E. L., Ellison, J., Duke, N. C. & Field, C. Threats to mangroves from climate change
554 and adaptation options: A review. *Aquatic Botany* **89**, 237-250 (2008).
- 555 39 Torio, D. D. & Chmura, G. L. Assessing Coastal Squeeze of Tidal Wetlands. *Journal of Coastal*
556 *Research*, 1049-1061 (2013).
- 557 40 Kirwan, M. L. *et al.* Limits on the adaptability of coastal marshes to rising sea level.
558 *Geophysical Research Letters* **37**, L23401 (2010).
- 559 41 D'Alpaos, A., Mudd, S. M. & Carniello, L. Dynamic response of marshes to perturbations in
560 suspended sediment concentrations and rates of relative sea level rise. *Journal of*
561 *Geophysical Research: Earth Surface* **116**, F04020 (2011).
- 562 42 French, J. Tidal marsh sedimentation and resilience to environmental change: Exploratory
563 modelling of tidal, sea-level and sediment supply forcing in predominantly allochthonous
564 systems. *Marine Geology* **235**, 119-136 (2006).
- 565 43 Kirwan, M. L. & Guntenspergen, G. R. Influence of tidal range on the stability of coastal
566 marshland. *Journal of Geophysical Research: Earth Surface* **115**, F02009 (2010).
- 567 44 Temmerman, S., Govers, G., Wartel, S. & Meire, P. Modelling estuarine variations in tidal
568 marsh sedimentation: response to changing sea level and suspended sediment
569 concentrations. *Marine Geology* **212**, 1-19 (2004).
- 570 45 Church, J. A. *et al.* in *Climate Change 2013: The Physical Science Basis. Contribution of*
571 *Working Group I to the Fifth Assessment Report of the Intergovernmental Panel on Climate*
572 *Change* (T.F. Stocker *et al.*) 1137-1216 (Cambridge University Press, 2013).
- 573 46 McFadden, L., Nicholls, R. J., Vafeidis, A. & Tol, R. S. J. Methodology for modeling coastal
574 space for global assessment. *Journal of Coastal Research* **23**, 911-920 (2007).
- 575 47 Jarvis, A., Reuter, H. I., Nelson, A. & Guevara, E. *Hole-Filled SRTM for the Globe Version 4*,
576 Available online: <http://srtm.csi.cgiar.org/> (2008).

577 48 Nicholls, R. J., Hoozemans, F. & Marchand, M. Increasing flood risk and wetland losses due to
578 global sea-level rise: regional and global analyses. *Global Environmental Change* **9**, 69 - 87
579 (1999).

580 49 Nicholls, R. J. Coastal flooding and wetland loss in the 21st century: changes under the SRES
581 climate and socio-economic scenarios. *Global Environmental Change* **14**, 69-86 (2004).

582 50 Muis, S., Verlaan, M., Winsemius, H. C., Aerts, J. C. J. H. & Ward, P. J. A global reanalysis of
583 storm surges and extreme sea levels. *Nature Communication* **7** (2016).

584 51 Titus, J. G. & Richman, C. Maps of lands vulnerable to sea level rise modeled elevations along
585 the US Atlantic and Gulf coasts. *Climate Research* **18**, 205-228 (2001).

586 52 Titus, J. G. & Wang, J. in *Background Documents Supporting Climate Change Science*
587 *Program Synthesis and Assessment Product 4.1 (EPA 430R07004)* (eds J.G. Titus & E.M.
588 Strange) (United States Environmental Protection Agency (EPA), 2008).

589 53 Vafeidis, A. T., Nicholls, R. J., McFadden, L., Hinkel, J. & Grasshoff, P. S. Developing a global
590 database for coastal vulnerability analysis: design issues and challenges. *The International*
591 *Archives of Photogrammetry, Remote Sensing and Spatial Information Sciences* **35**, 801-805
592 (2004).

593 54 Balke, T., Stock, M., Jensen, K., Bouma, T. J. & Kleyer, M. A global analysis of the seaward salt
594 marsh extent: The importance of tidal range. *Water Resources Research* **52**, 3775-3786
595 (2016).

596 55 Ellison, J. in *Coastal Wetlands: An Integrated Ecosystem Approach* (eds. Perillo, E. Wolanski,
597 D. Cahoon, & M. Brinson) 565-591 (Elsevier, 2009).

598 56 McIvor, A. L., Spencer, T., Möller, I. & M., S. *The response of mangrove soil surface elevation*
599 *to sea level rise*. (The Nature Conservancy and Wetlands International 2013).

600 57 McKee, K. L. & Patrick, W. H. The relationship of smooth cordgrass (*Spartina alterniflora*) to
601 tidal datums: a review. *Estuaries* **11**, 143-151 (1988).

602 58 Odum, W. E. Comparative ecology of tidal freshwater and salt marshes. *Annual Review of*
603 *Ecology and Systematics* **19**, 147-176 (1988).

604 59 Gray, A. J., Marshall, D. F., Raybould, A. F., M. Begon, A. H. F. & Macfadyen, A. in *Advances in*
605 *Ecological Research* Vol. 21 (eds. Begon, M., Fitter, A. & Macfadyen, A.) 1-62 (Academic
606 Press, 1991).

607 60 Jones, C. D. *et al.* The HadGEM2-ES implementation of CMIP5 centennial simulations.
608 *Geoscientific Model Development* **4**, 543 (2011).

609 61 Peltier, W. Global glacial isostasy and the surface of the ice-age earth: The ice-5G (VM2)
610 model and grace. *Annual Review of Earth and Planetary Sciences* **32**, 111-149 (2004).

611 62 Meckel, T. A., Ten Brink, U. S. & Williams, S. J. Sediment compaction rates and subsidence in
612 deltaic plains: numerical constraints and stratigraphic influences. *Basin Research* **19**, 19-31
613 (2007).

614 63 Syvitski, J.P.M. Deltas at risk. *Sustainability Science* **3**, 23-32 (2008).

615 64 Ericson, J. P., Vörösmarty, C. J., Dingman, S. L., Ward, L. G. & Meybeck, M. Effective sea-level
616 rise and deltas: causes of change and human dimension implications. *Global Planetary*
617 *Change* **50**, 63-82 (2006).

618 65 Pickering, M. D. *et al.* The impact of future sea-level rise on the global tides. *Continental*
619 *Shelf Research* **142**, 50-68 (2017).

620 66 Egbert, G. D., Ray, R. D. & Bills, B. G. Numerical modeling of the global semidiurnal tide in the
621 present day and in the last glacial maximum. *Journal of Geophysical Research: Oceans* **109**,
622 C03003 (2004).

623 67 Center for International Earth Science Information Network - CIESIN - Columbia University,
624 International Food Policy Research Institute - IFPRI, The World Bank & Centro Internacional
625 de Agricultura Tropical - CIAT. *Global Rural-Urban Mapping Project, Version 1 (GRUMPv1):*
626 *Population Density Grid*, Available online: <http://dx.doi.org/10.7927/H4R20Z93> (2011).

627 68 Fricko, O. *et al.* The marker quantification of the Shared Socioeconomic Pathway 2: A
628 middle-of-the-road scenario for the 21st century. *Global Environmental Change* **42**, 251-267
629 (2017).

630 69 Barrot, G., Mangin, A. & Pinnock, S. *Global Ocean Colour for Carbon Cycle Research, Product*
631 *User Guide*. (ACRI-ST, 2007).

632 70 Raabe, E. A. & Stumpf, R. P. Expansion of Tidal Marsh in Response to Sea-Level Rise: Gulf
633 Coast of Florida, USA. *Estuaries and Coasts* **39**, 145-157 (2016).

634 71 Schieder, N. W., Walters, D. C. & Kirwan, M. L. Massive Upland to Wetland Conversion
635 Compensated for Historical Marsh Loss in Chesapeake Bay, USA. *Estuaries and Coasts* (2017).

636 72 Smith, J. A. M. The Role of Phragmites australis in Mediating Inland Salt Marsh Migration in a
637 Mid-Atlantic Estuary. *PLOS ONE* **8**, e65091 (2013).

638 73 Langston, A. K., Kaplan, D. A. & Putz, F. E. A casualty of climate change? Loss of freshwater
639 forest islands on Florida's Gulf Coast. *Global Change Biology* **23**, 5383-5397 (2017).

640 74 Anisfeld, S. C., Cooper, K. R. & Kemp, A. C. Upslope development of a tidal marsh as a
641 function of upland land use. *Global Change Biology* **23**, 755-766 (2017).

642 75 Feagin, R. A., Martinez, M. L., Mendoza-Gonzalez, G. & Costanza, R. Salt marsh zonal
643 migration and ecosystem service change in response to global sea level rise: a case study
644 from an urban region. *Ecology and Society* **15**, 14 (2010).

645 76 Gilman, E., Ellison, J. & Coleman, R. Assessment of Mangrove Response to Projected Relative
646 Sea-Level Rise And Recent Historical Reconstruction of Shoreline Position. *Environmental*
647 *Monitoring and Assessment* **124**, 105-130 (2007).

648 77 Nitto, D. D. *et al.* Mangroves facing climate change: landward migration potential in
649 response to projected scenarios of sea level rise. *Biogeosciences* **11**, 857-871 (2014).

650 78 Rogers, K., Saintilan, N. & Copeland, C. Managed Retreat of Saline Coastal Wetlands:
651 Challenges and Opportunities Identified from the Hunter River Estuary, Australia. *Estuaries*
652 *and Coasts* **37**, 67-78 (2014).

653 79 Stralberg, D. *et al.* Evaluating Tidal Marsh Sustainability in the Face of Sea-Level Rise: A
654 Hybrid Modeling Approach Applied to San Francisco Bay. *PLOS ONE* **6**, e27388 (2011).

655 80 Craft, C., Broome, S. & Campbell, C. Fifteen Years of Vegetation and Soil Development after
656 Brackish-Water Marsh Creation. *Restoration Ecology* **10**, 248-258 (2002).

657 81 Mossman, H. L., Brown, M. J. H., Davy, A. J. & Grant, A. Constraints on Salt Marsh
658 Development Following Managed Coastal Realignment: Dispersal Limitation or
659 Environmental Tolerance? *Restoration Ecology* **20**, 65-75 (2012).

660 82 Mossman, H. L., Davy, A. J. & Grant, A. Does managed coastal realignment create
661 saltmarshes with 'equivalent biological characteristics' to natural reference sites? *Journal of*
662 *Applied Ecology* **49**, 1446-1456 (2012).

663 83 Wolters, M., Garbutt, A., Bekker, R. M., Bakker, J. P. & Carey, P. D. Restoration of salt-marsh
664 vegetation in relation to site suitability, species pool and dispersal traits. *Journal of Applied*
665 *Ecology* **45**, 904-912 (2008).

666 84 Nicholls, R. J. *et al.* Stabilization of global temperature at 1.5°C and 2.0°C: implications for
667 coastal areas. *Philosophical Transactions of the Royal Society A: Mathematical, Physical and*
668 *Engineering Sciences* **376** (2018).

669 85 Song, J., Fu, X., Wang, R., Peng, Z.-R. & Gu, Z. Does planned retreat matter? Investigating
670 land use change under the impacts of flooding induced by sea level rise. *Mitigation and*
671 *Adaptation Strategies for Global Change* (2017).

672 86 Sadoff, C. W. *et al.* *Securing Water, Sustaining Growth: Report of the GWP/OECD Task Force*
673 *on Water Security and Sustainable Growth*. (University of Oxford, 2015).

674 87 Mittermeier, R. A. *et al.* Wilderness and biodiversity conservation. *Proceedings of the*
675 *National Academy of Sciences* **100**, 10309-10313 (2003).

- 676 88 Abel, N. *et al.* Sea level rise, coastal development and planned retreat: analytical framework,
677 governance principles and an Australian case study. *Environmental Science & Policy* **14**, 279-
678 288 (2011).
- 679 89 Kousky, C. Managing shoreline retreat: a US perspective. *Climatic Change* **124**, 9-20 (2014).
- 680 90 Field, C. R., Dayer, A. A. & Elphick, C. S. Landowner behavior can determine the success of
681 conservation strategies for ecosystem migration under sea-level rise. *Proceedings of the*
682 *National Academy of Sciences* **114**, 9134-9139 (2017).
- 683 91 The Organisation for Economic Co-operation and Development - OECD. *OECD Regional*
684 *Typology*. (OECD, 2011).

685 **Code availability**

686 The computer code that supports the findings of this study is available for non-commercial use (CC
687 BY-NC-SA 4.0) from the GitLab repository “global-coastal-wetland-model”,
688 <https://gitlab.com/mark.schuerch/global-coastal-wetland-model.git>.

689 **Data availability**

690 The data that support the findings of this study are available from the corresponding author upon
691 reasonable request. The source data for figures 1 and ED2 are provided with the paper.

692 **Extended Data figure and table legends**

693 ED Figure 1: Map of model performance during model calibration. Green lines indicate segments
694 where the modelled sediment balances match the observed trends in wetland elevation change
695 relative to sea level rise^{3,4,19}. Red segments indicate model mismatches. The frequency distributions
696 for total suspended matter (TSM) and tidal range (TR) display the distributions of both parameters in
697 matching (green bars) and mismatching segments (red bars), and how they compare to the overall
698 frequency distributions of both parameters (blue bars). The overall frequency distribution only
699 includes coastline segments where coastal wetlands are present. The displayed coastline was
700 generated during the DINAS-COAST FP5-EESD EU project (EVK2-CT-2000-00084).

701 ED Figure 2: Global change (km²) in coastal wetland area. Results for all three SLR scenarios (RCP 2.6
702 - low, RCP 4.5 - medium, RCP 8.5 - high) and a total of eight different model configurations. These
703 include the upper and lower boundaries of the BAU (5, 20 people km⁻²) and the upper boundaries of

704 the NB 1 and NB 2 scenarios (150 and 300 people km⁻²) as defined in ED Table2 (solid lines). The
705 dashed lines represent the four hypothetical scenarios, as characterized in ED Table2: (i) “wetland
706 migration only”, (ii) “sediment accretion only”; (iii) “maximum resilience” and (iv) “no resilience”.

707 ED Figure 3: Spatial distribution of coastal wetland change. Absolute (a) and relative (b) changes in
708 coastal wetland areas are displayed for a medium SLR scenario (RCP4.5 - med)), assuming the
709 possibility of wetland inland migration everywhere, but in urban areas with a population density
710 >300 people km⁻². Population density is subject the population growth throughout the simulation
711 period, following the socio-economic pathway SSP2^{20,68}. The displayed coastline was generated
712 during the DINAS-COAST FP5-EESD EU project (EVK2-CT-2000-00084).

713 ED Figure 4: Flow diagram representing the overall structure of the global coastal wetland model.
714 Input parameters are shown on the left, output parameters on the right. “Net wetland change”
715 equals “Inland wetland gain” minus “Seaward wetland loss”.

716 ED Figure 5: Schematization of topographic profiles. The conversion of upland areas to coastal
717 wetlands (if not inhibited by anthropogenic barriers) and the unconstrained seaward loss of coastal
718 wetlands in response to sea level rise is shown for an exemplary coastline segment (in western
719 France). Inundation of terrestrial uplands follows the rising mean high water spring (MHWS) level
720 between the time steps t1 and t2 (blue), whereas the unconstrained seaward loss follows the
721 increase in mean sea level (MSL) when neglecting sediment accretion processes (red). To improve
722 the clarity of the figure the actual MHWS level (2.54 m) and MSL rise are exaggerated.

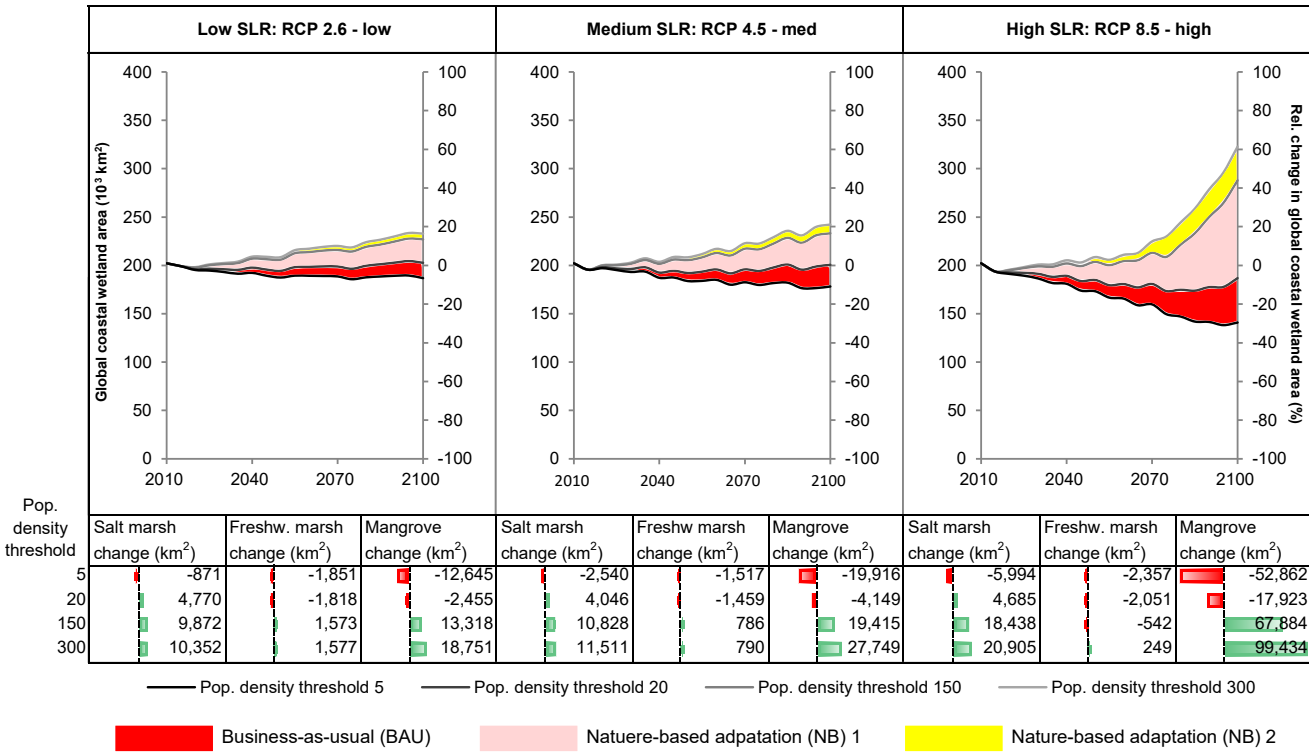
723 ED Figure 6: Map of regionalized relative sea level rise (m). Total relative sea level rise for the
724 medium SLR scenario (ED Table2) during the simulation period, including a delta subsidence rate of 2
725 mm yr⁻¹ (2010-2100). Black coastlines indicate regions of RLSR similar to the global mean. The
726 displayed coastline was generated during the DINAS-COAST FP5-EESD EU project (EVK2-CT-2000-
727 00084).

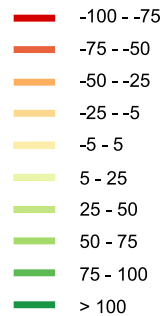
728 ED Table 1: Performance of calibrated model when compared to field data^{3,4,19}. Summary of
729 comparison between locally measured sediment balance^{3,4} for marshes and mangrove systems¹⁹ and
730 modelled trends derived from the calculated WAS using $m_{TM}=3.42$, $m_{Man}=4.42$, $iTF=1.5$, $i_{Man}=0$,
731 $e_{TF}=0.915$, $e_{Man}=1.18$ and $a=40 \text{ mg l}^{-1}$. “Model fit” represents the number of segments, where the
732 calculated WAS corresponds with the measured sediment category.

733 ED Table 2: Characteristics of the employed scenarios. Three sea level rise (SLR) scenarios (RCP 2.6 –
734 low, RCP 4.5 – med, RCP 8.5 – high) were combined with three human adaptation scenarios
735 (business-as-usual: BAU; moderate nature-based adaptation: NB 1; and extreme nature-based
736 adaptation: NB 2), accounting for varying degrees of accommodation space available for coastal
737 wetlands, and four hypothetical scenarios (HYS 1: wetland migration only, HYS 2: sediment accretion
738 only, HYS 3: maximum resilience, HYS 4: no resilience), used to quantify the contribution of vertical
739 sediment accretion and horizontal inland migration to the overall resilience of coastal wetlands to
740 global SLR (sensitivity analysis).


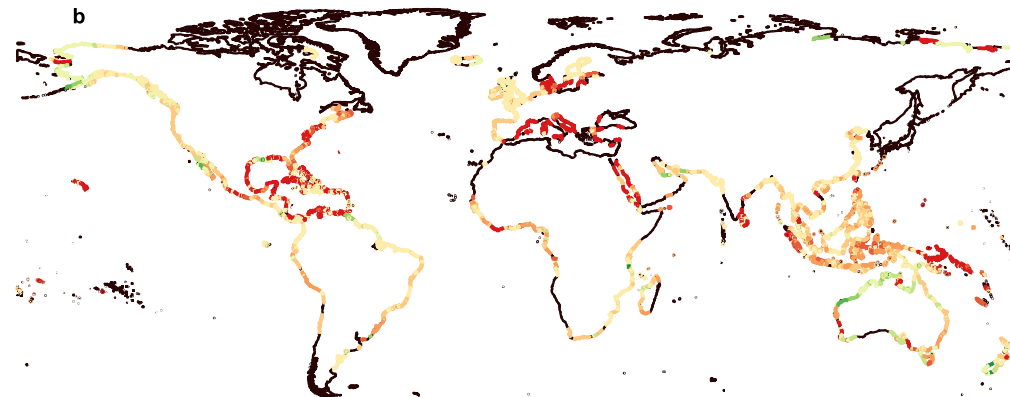
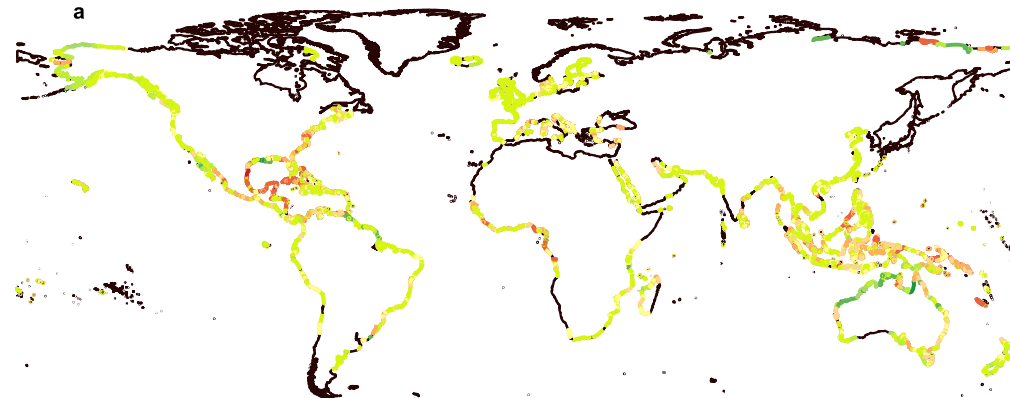
741 ED Table 3: Model sensitivity to variations in sediment availability. Percent deviations in total global
742 wetland area by 2100 from simulations with current-day sediment availability for all four population
743 density thresholds (ED Table2) and reductions/increases of the constant sediment supply by 50%
744 and 20%.

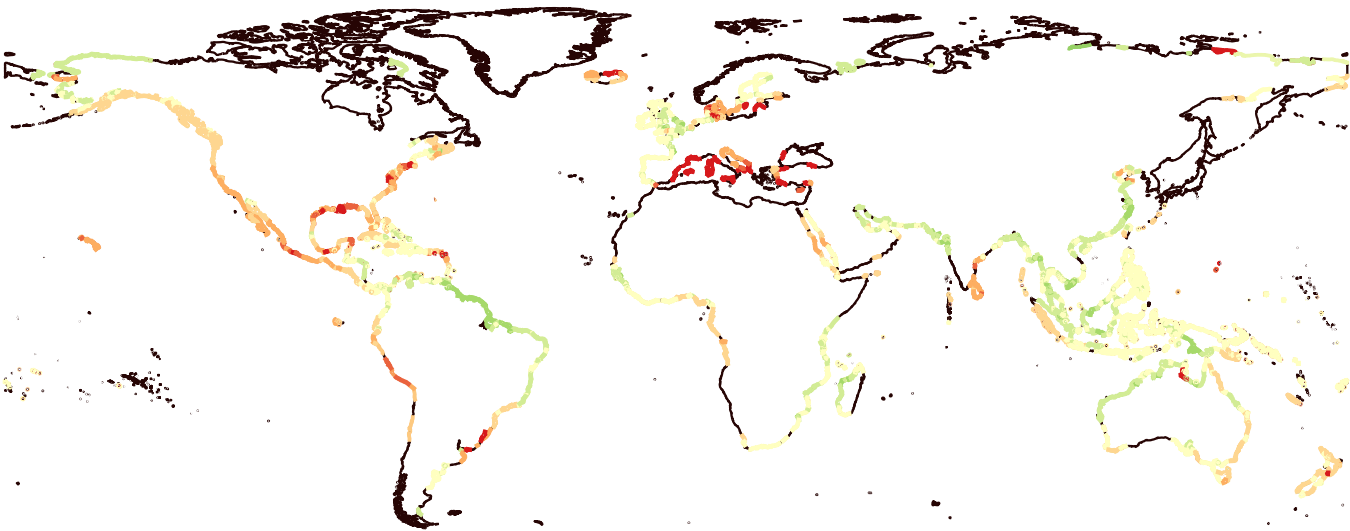
745 ED Table 4: Model sensitivity to variations in natural and human-induced delta subsidence. Percent
746 gain (positive) and loss (negative) of total global wetland area by 2100 from simulations for all four
747 population density thresholds (ED Table2) and three different rates for uniform delta subsidence for
748 all 117 deltas listed in the DIVA database³¹.



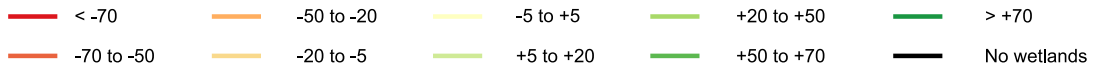
aAbsolute wetland change (km²)**b**Relative wetland change (km²)

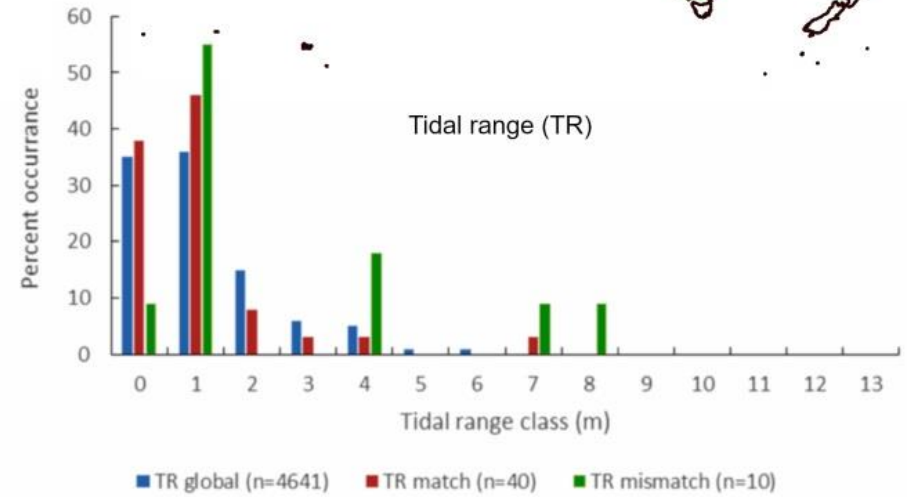
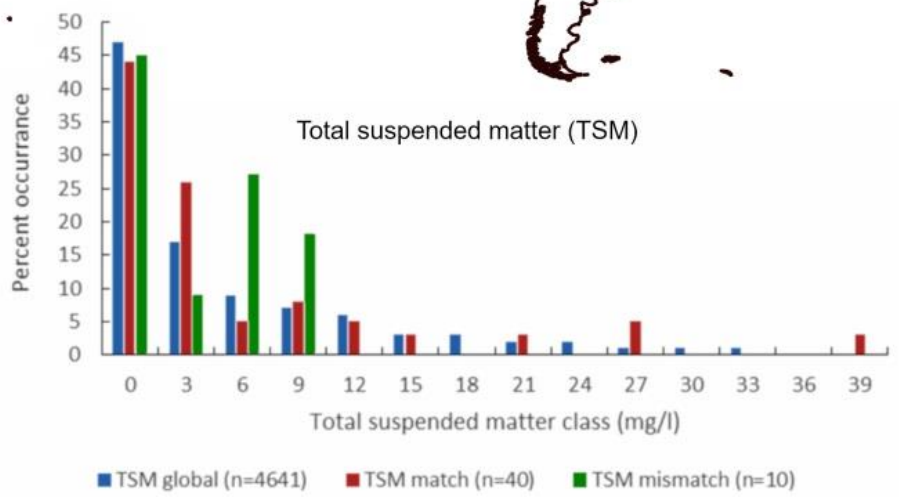
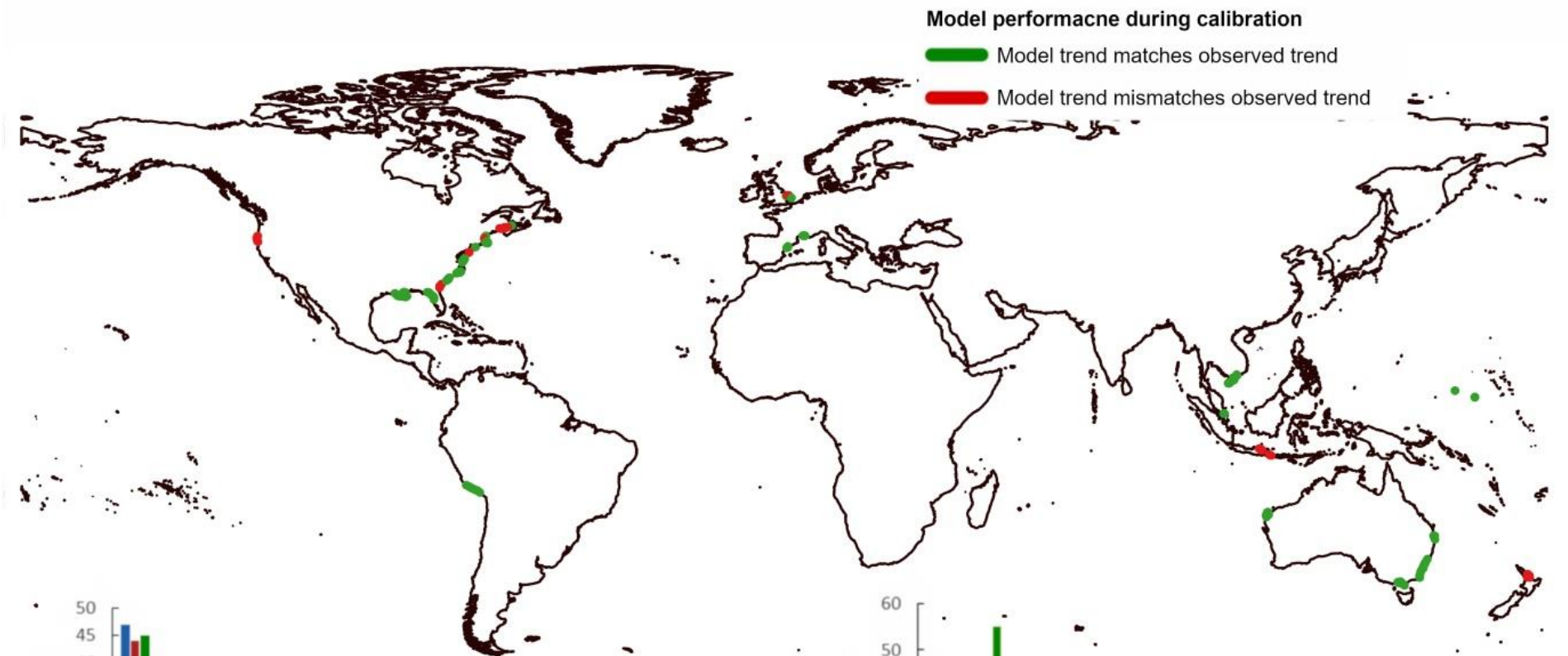
Coastline

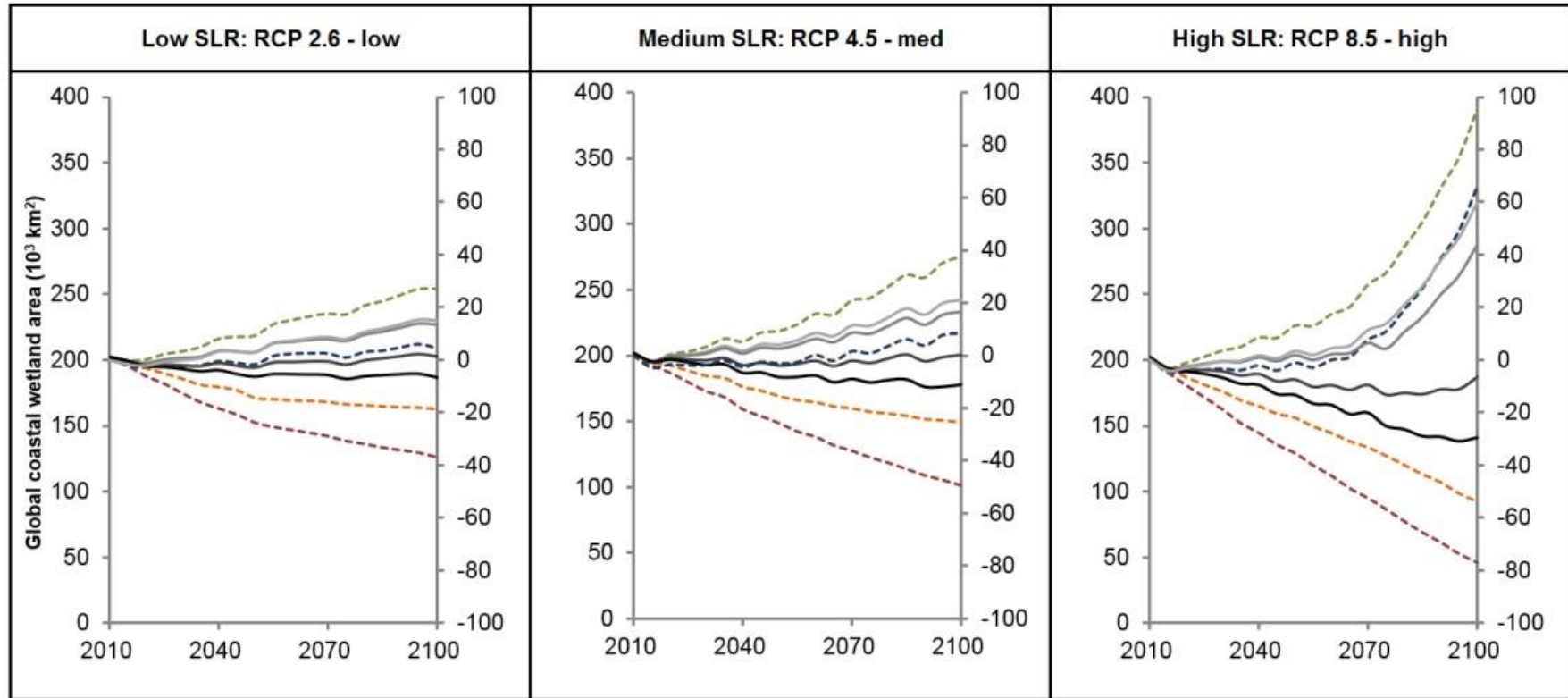
 No wetlands



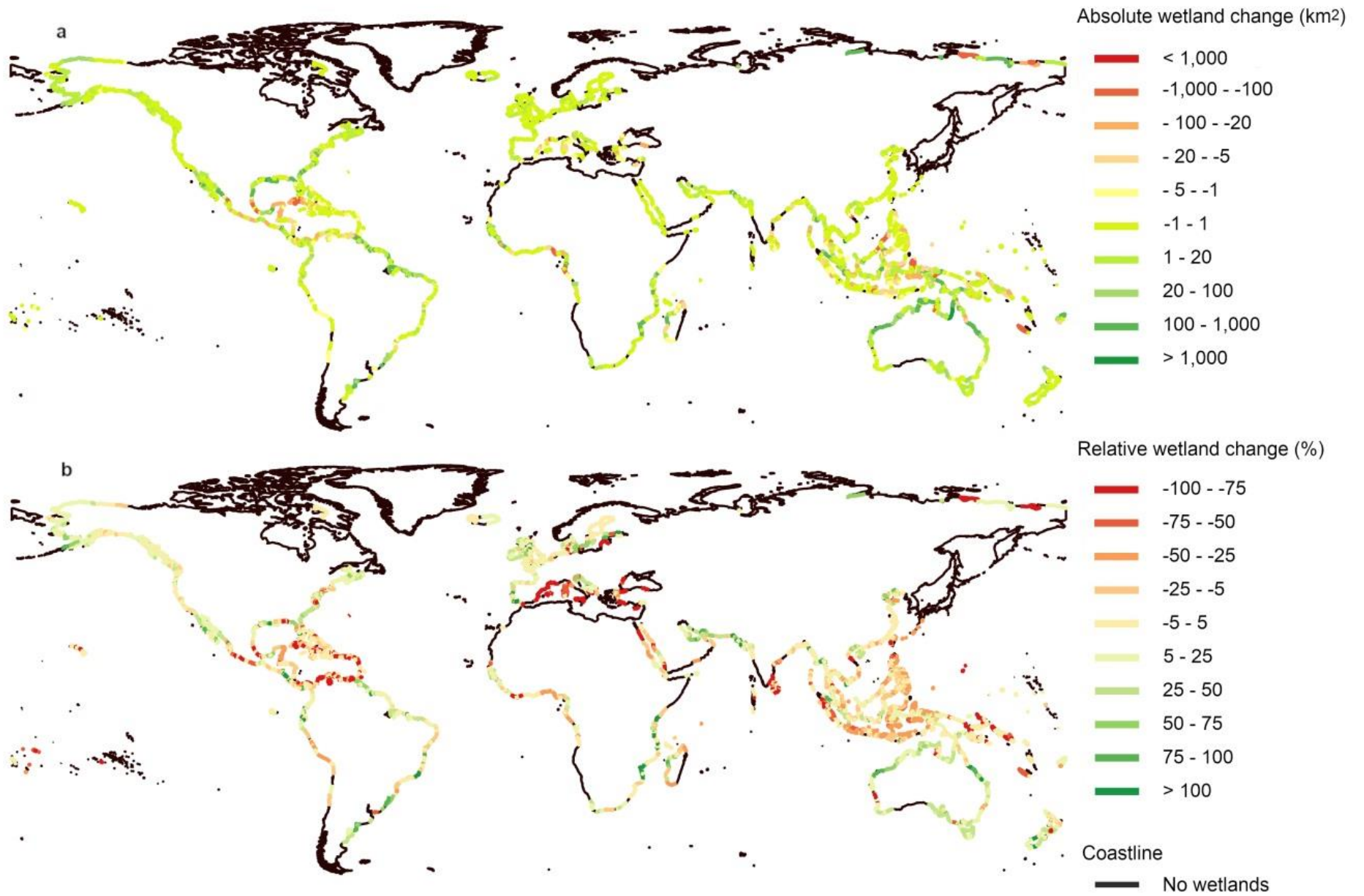
Present sediment balance (mg/l): Sediment deficite (negative), sediment surplus (positive)

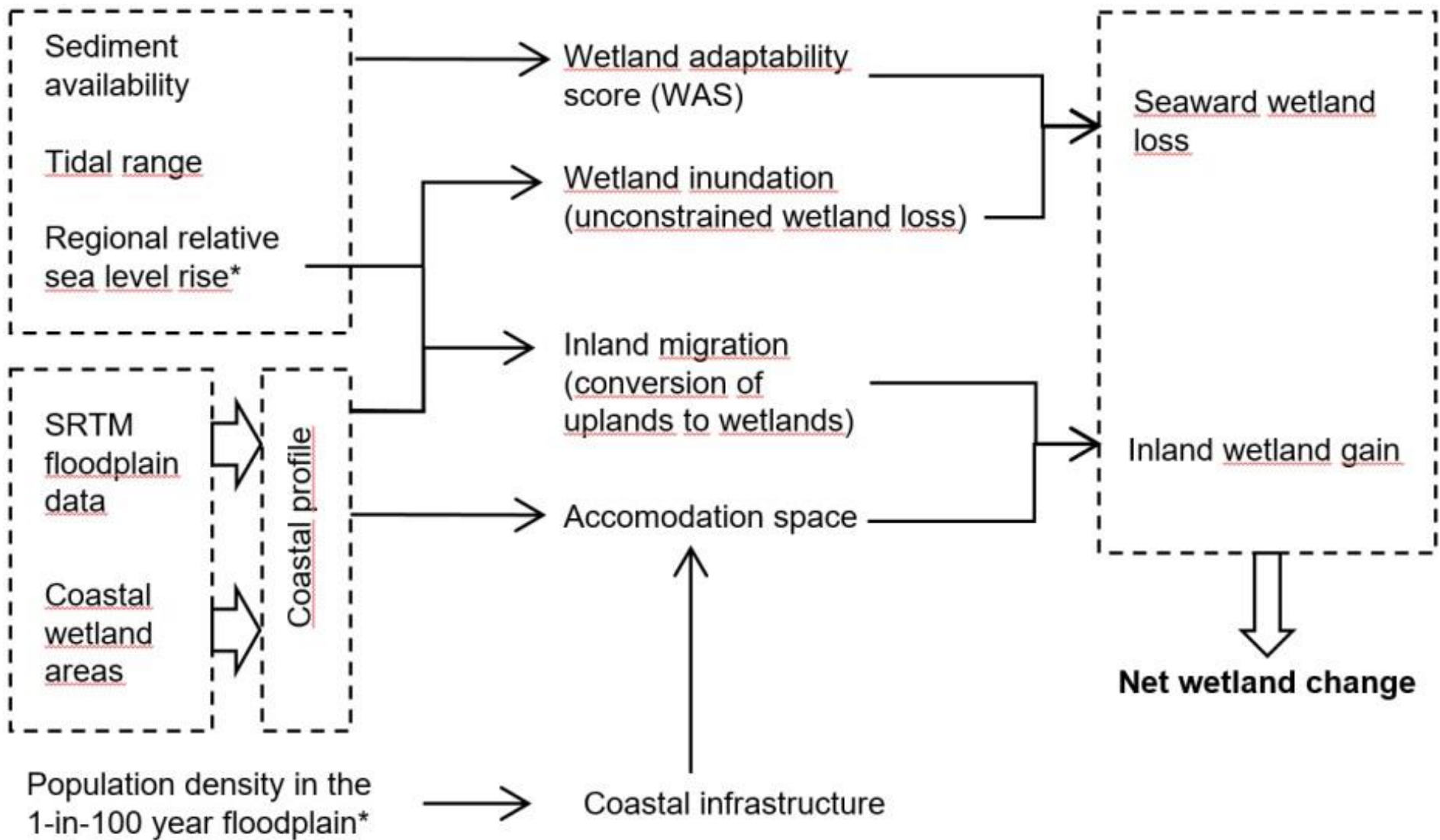




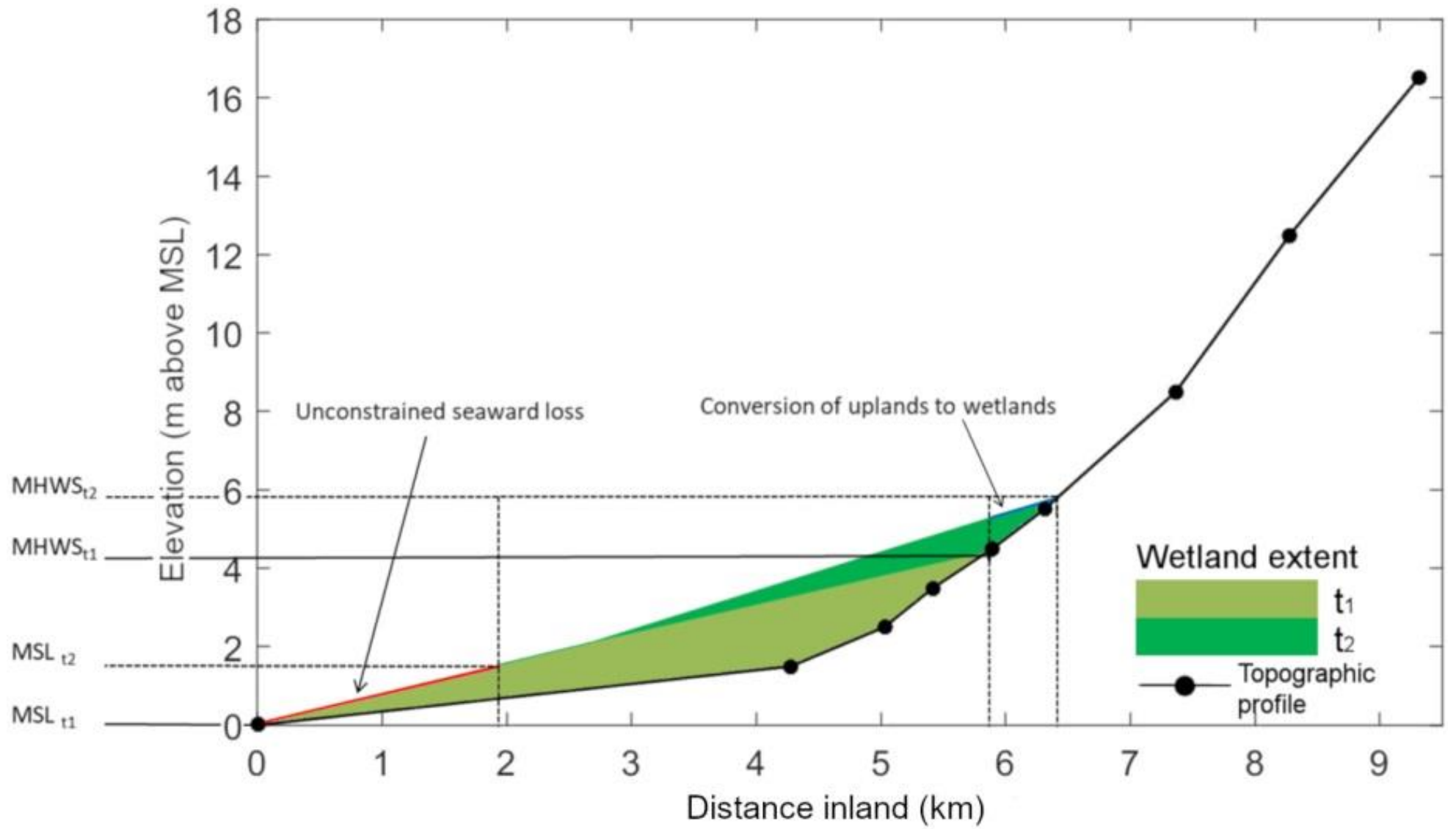


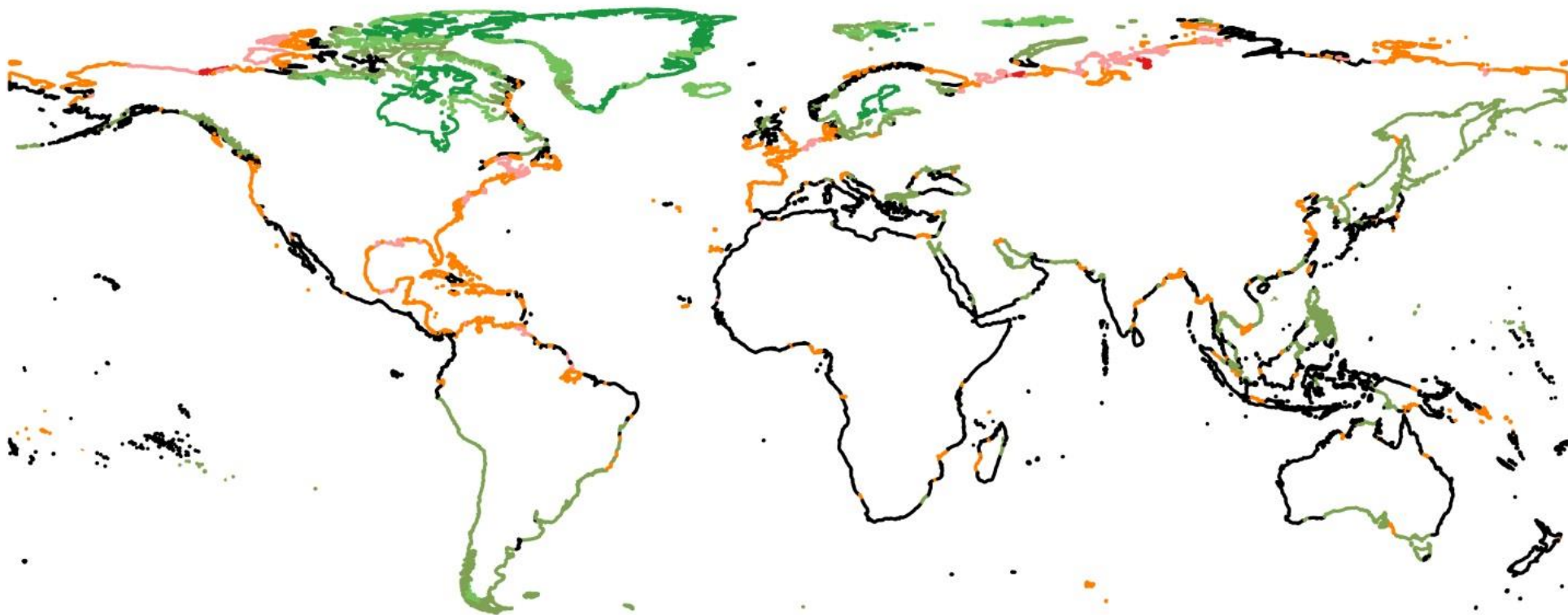
- - - - - Maximum resilience (HYS 3)
- - - - - Wetland migration only (HYS 1)
- - - - - Sediment accretion only (HYS 2)
- - - - - No resilience (HYS 4)
- — — — — Pop. density threshold 300
- — — — — Pop. density threshold 150
- — — — — Pop. density threshold 20
- — — — — Pop. density threshold 5





*Dynamic model variable, subject to projection until 2100





Relative sea level rise until 2100



	Category (defined based on the field measurements)	Categorization of Field measurements	WAS	Model fit (number of segments)	Total occurrences (number of segments)
Tidal marshes	Total model fit	All data	All data	16	23
	"elevation deficit"	< -2 mm yr ⁻¹	<-1	3	5
	"balanced"	-2 to 2 mm yr ⁻¹	-1 to 1	10	10
	"elevation surplus"	> 2 mm yr ⁻¹	>1	3	8
Mangrove systems	Total model fit	All data	All data	20	23
	"elevation deficit"	< -2 mm yr ⁻¹	<-1	12	12
	"balanced"	-2 to 2 mm yr ⁻¹	-1 to 1	6	6
	"elevation surplus"	> 2 mm yr ⁻¹	>1	2	5

SLR scenario	Land-ice contribution	SLR until 2100 (cm)	Accommodation space scenario		Population density threshold (people km ⁻²)		Sediment accretion	
					Lower boundary	Upper boundary		
Low: RCP 2.6 (5%)	low	29	Human adaptation scenarios	BAU*	BAU	5	20	Yes
				NB†	NB 1	20	150	
				NB†	NB 2	150	300	
			4 Hypothetical scenarios (HYS)	HYS 1	∞‡	∞‡	No	
				HYS 2	0§	0§	Yes	
				HYS 3	∞‡	∞‡	Yes	
				HYS 4	0§	0§	No	
Medium: RCP 4.5 (50%)	medium	50	Human adaptation scenarios	BAU*	BAU	5	20	Yes
				NB†	NB 1	20	150	
				NB†	NB 2	150	300	
			4 Hypothetical scenarios (HYS)	HYS 1	∞‡	∞‡	No	
				HYS 2	0§	0§	Yes	
				HYS 3	∞‡	∞‡	Yes	
				HYS 4	0§	0§	No	
High: RCP 8.5 (95%)	high	110	Human adaptation scenarios	BAU*	BAU	5	20	Yes
				NB†	NB 1	20	150	
				NB†	NB 2	150	300	
			4 Hypothetical scenarios (HYS)	HYS 1	∞‡	∞‡	No	
				HYS 2	0§	0§	Yes	
				HYS 3	∞‡	∞‡	Yes	
				HYS 4	0§	0§	No	

*BAU: Business-as-usual scenario

†NB: Nature-based adaptation scenarios

‡Population density threshold = ∞: Unlimited accommodation space

§Population density threshold = 0: No accommodation space

Human adaptation scenario	Population density threshold (people km ⁻²)	Sediment availability (constant in time)	RCP 2.6 - low (percent)	RCP 4.5 - medium (percent)	RCP 8.5 - high (percent)
Nature-based adaptation 2 – upper boundary	300	-50%	-2.9	-4.3	-6.5
		-20%	-1.1	-1.6	-2.5
		+20%	0.9	1.4	2.7
		+50%	2.5	3.5	6.1
Nature-based adaptation 2 – lower boundary = Nature-based adaptation 1 – upper boundary	150	-50%	-2.9	-4.3	-6.4
		-20%	-1.1	-1.6	-2.5
		+20%	0.9	1.4	2.7
		+50%	2.5	3.5	6.0
Nature-based adaptation 1 – lower boundary = Business-as-usual – upper boundary	20	-50%	-2.8	-4.1	-6.0
		-20%	-1.0	-1.5	-2.3
		+20%	0.9	1.3	2.5
		+50%	2.3	3.4	5.7
Business-as-usual – lower boundary	5	-50%	-2.7	-3.9	-5.7
		-20%	-1.0	-1.4	-2.2
		+20%	0.9	1.3	2.3
		+50%	2.3	3.3	5.3

Model setup	Delta subsidence (mm yr ⁻¹)	RCP 2.6 - 5% (percent)	RCP 4.5 - 50% (percent)	RCP 8.5 - 95% (percent)
Pop. density threshold 300	0	14.0	18.7	55.8
Pop. density threshold 150		11.4	14.8	39.5
Pop. density threshold 20		0.1	-1.0	-10.2
Pop. density threshold 5		-6.7	-10.6	-31.3
Pop. density threshold 300	2	15.2	19.8	59.7
Pop. density threshold 150		12.3	15.3	42.4
Pop. density threshold 20		0.2	-0.8	-7.6
Pop. density threshold 5		-7.6	-11.9	-30.3
Pop. density threshold 300	5	16.7	21.5	62.7
Pop. density threshold 150		12.8	15.5	44.1
Pop. density threshold 20		0.5	1.2	-6.3
Pop. density threshold 5		-9.6	-14.6	-31.0

Mark Schuerch^{1,2*}, Tom Spencer², Stijn Temmerman³, Matthew L. Kirwan⁴, Claudia Wolff⁵, Daniel Lincke⁶, Chris J. McOwen⁷, Mark D. Pickering⁸, Ruth Reef⁹, Athanasios T. Vafeidis⁵, Jochen Hinkel^{6,10}, Robert J. Nicholls¹¹, Sally Brown¹¹

¹ Lincoln Centre for Water and Planetary Health, School of Geography, University of Lincoln, Lincoln, United Kingdom

² Cambridge Coastal Research Unit, Department of Geography, University of Cambridge, Cambridge United Kingdom ³ Ecosystem Management Research Group, University of Antwerp, Antwerp, Belgium

⁴ Virginia Institute of Marine Science, College of William and Mary, Gloucester Point, Virginia, USA

⁵ Institute of Geography, Christian-Albrechts University of Kiel, Kiel, Germany

⁶ Global Climate Forum, Berlin, Germany

⁷ UN Environment World Conservation Monitoring Centre, Cambridge, United Kingdom

⁸ Ocean and Earth Science, National Oceanography Centre, University of Southampton, Southampton, United Kingdom

⁹ School of Earth, Atmosphere and Environment, Monash University, Clayton, Victoria, Australia

¹⁰ Division of Resource Economics, Thae-Institute and Berlin Workshop in Institutional Analysis of Social-Ecological Systems (WINS), Humboldt-University, Berlin, Germany

¹¹ Faculty of Engineering and the Environment, University of Southampton, Southampton, United Kingdom

*Corresponding author: mschuerch@lincoln.ac.uk

Future response of global coastal wetlands to sea level rise

Supplementary Methods

The tidal range model

Our new tidal dataset^{65,92} was generated using OTISmpi⁶⁶, a forward global tidal model, solving the non-linear shallow water equations on a C-grid using a finite differences time stepping method. The employed model setup is optimised to reconstruct shelf tides in order to assess tidal changes at major coastal port city locations around the world. The model outputs are comparable in accuracy to operational regional tidal models used to forecast tides and surge water levels at the coastline⁶⁵. This purely physics based prognostic model setup was shown to have good skills at representing the present-day tides with an RMS error of 0.10 m globally, 0.21 m for shelf seas (<200 m) and 0.09 m in deep water (>200m)⁹² when compared with the FES2004 tidal atlas solutions⁹³. Additionally, as the prognostic model skill is not based on assimilation of any present-day observations, it can be used to assess changes to the tides with SLR and coastal adaptation.

OTISmpi was forced with the M2, S2, K1 and O1 dominant global tidal constituents and included iterative corrections for self-attraction and loading, as well as an internal wave drag parameterisation. The model was run for 50 days with the last 20 days used in the harmonic analysis to ensure that it had fully spun up and tidal constituents could be properly separated. All tidal parameters were derived from a 15-day sea-level reconstruction based on the four modelled tidal constituents; this time series included the spring HW peaks (semidiurnal regions) and tropical HW peaks (diurnal regions), it did not include longer term variability such as the equinoctial or nodal

tides. MLW, MHW and MHW were derived using a novel percentile method on the water level time series which enabled a spatially coherent field for these parameters across semidiurnal, diurnal and mixed tidal regimes^{65,92}. The optimal percentiles derived were 10.8, 71.3 and 88.8 respectively with the mean taken of values +/-1%ile around each to provide a smooth field. Given the constituents used in the time series reconstruction, its length and the variety of tidal regimes the best method to estimate MHW was to take the maximum of the 15-day time series.

The gridded tidal data ($1/8^\circ \times 1/8^\circ$) was projected to each coastline segment by calculating the average of all grid cells intersecting the segment. If no grid cells crossed a segment (which is common around semi-enclosed seas), the nearest neighbour method was used. It should be noted that here we assume the tides to remain constant throughout the simulation period, although we acknowledge that SLR and coastal adaptation strategies, being dynamic variables within the model, may affect the tide itself⁶⁵.

Calibration procedure

The model parameters m , e , i and a (eqs. 3+4) are estimated using the following stepwise calibration procedure:

- (i) Derivation of the coefficients m , i and e from the model ensemble runs presented by Kirwan et al.⁴⁰. These coefficients are assumed to be valid for segments, where tidal marshes (tidal salt and freshwater marshes) are present and in the following referred to as m_{TM} , i_{TF} and e_{TF} .
- (ii) Determination of model parameter a by comparing the modelled WAS with field measurements of elevation deficit/surplus on salt marshes derived from Sedimentation-Erosion Tables (SET), a widespread and standardized method for measuring the vertical elevation growth of coastal wetlands^{94,95}. This dataset was compiled from meta-data analyses by Kirwan et al.⁴ and Crosby et al.³ and includes measurements of vertical marsh elevation changes from 57 marsh sites across Europe, Australia and North America. The majority of the data originates from the US East coast. We use the local RSLR rate reported by Kirwan et al.⁴ and Crosby et al.³ in combination with the tidal range data derived from Pickering et al.⁹² to calculate the WAS for every coastline segment (eq. 3+4), where field measurements are available. Measured accretion deficits/surplus as well as the local RSLR rates are aggregated to the DIVA coastline segments by averaging all values within one segment.

The field measurements and the calculated WAS are divided into the three categories “sediment deficit”, “balanced”, “sediment surplus” (according to Suppl. Table 1) and the value of a in eq. 4 is changed such that the number of segments, where the model correctly estimates the measured category is maximized (“model fit”).

- (iii) Adoption of the model coefficients m_{TF} , e_{TF} and i_{TF} for mangrove systems. The model parameters are optimised by comparing the segment specific WAS, using the model parameter a , as determined in step (i), with the elevation change data presented by Lovelock et al.¹⁹. We thereby apply the exact same procedure as described in step (ii) except that m_{Man} , e_{Man} and i_{Man} are calibrated instead of a . In contrast to the model parameters m_{TF} , e_{TF} and i_{TF} the model parameters m_{Man} , e_{Man} and i_{Man} have to be calibrated against reported elevation data¹⁹ as the ensemble model results by Kirwan et al.⁴⁰ are only applicable for tidal marshes, and no comparable study has been conducted for mangrove systems. Same as the data published by Kirwan et al.⁴ and Crosby et al.³, the data presented by Lovelock et al.¹⁹ were assessed by SET measurements in 24 mangrove systems distributed across Southeast Asia and Australia.

The best model fit was achieved with $m_{TM}=3.42$, $m_{Man}=4.42$, $i_{TF}=-1.5$, $l_{Man}=0$, $e_{TF}=0.915$, $e_{Man}=1.18$ and $\alpha=40 \text{ mg l}^{-1}$. Suppl. Table 1 shows that during the final calibration run the model is well able to reproduce segments that are “balanced” or face a “sediment deficit”, whereas the model performance in segments with a “sediment surplus” is lower. This bias implies that the model is more likely to underestimate the adaptive capacity of coastal wetlands, potentially resulting in an underestimation of the modelled global wetland areas.

Estimation of current-day coastal protection level

In order to define the population density thresholds for the upper and lower boundaries of our business-as-usual human adaptation scenario, which we assume to be representative of the current-day accommodation space of coastal wetlands, we define the population density threshold that corresponds to the proportion of the current-day coastline being protected by coastal sea defences as the upper limit. This assumption seems reasonable as inland migration of coastal wetlands is surely inhibited by coastal sea defences, but also by other coastal infrastructure, such as roads, railways and other impervious surfaces^{18,96}.

We therefore model the global distribution of coastal sea defences according the current state of the art and compare the percentage of globally protected coastline with the respective percentage, if the dike building decision is only based on local population density. The construction of coastal sea defences has been suggested to be related to the economic status of a region. Hinkel et al.³², for example, use the national Gross Domestic Product (GDP) and population density to globally model the distribution of coastal sea defences. Similarly, Sadoff et al.⁸⁶ suggest protection levels to vary between poor and rich countries, with rich countries protecting sparser populated areas than poor countries. They suggest that countries with a Gross National Income (GNI) per capita of $\leq \$4085$, defined as low and medium low-income countries by the United Nations⁹⁷, only protect their urban areas from coastal flooding, whereas richer countries (GNI per capita of $> \$4085$) also protect their rural areas. While Sadoff et al.⁸⁶ do not give a definition for rural and urban, such definitions are given by the European Commission²², who defines urban areas to be areas with population densities $> 300 \text{ people km}^{-2}$.

Under the assumption that the Gross Domestic Product (GDP) is comparable to the GNI^{98,99}, we use the GDP per capita and the population densities from Hinkel et al.³² to model the global extent of coastal sea defences as suggested by Sadoff et al.⁸⁶. We calculate the proportion of coasts globally that are protected by a coastal sea defence structure and compare this proportion with the corresponding proportion when modelling the extent of coastal sea defences using a range of population densities as a sole criteria (not considering GDP or GNI). The global proportion of protected coastline, using the GDP-population model by Sadoff et al.⁸⁶ is 41.97%. In comparison, the global proportion of protected coastline modelled with a population density threshold of 20 people km^{-2} (without considering GDP) is 41.90%. We therefore conclude that the present-day coastal protection level is best represented by a threshold population density of 20 people km^{-2} , which at the same time constitutes the upper boundary of our business-as-usual (BAU) scenario. For the lower boundary of the BAU scenario, we use a population density threshold of 5 people km^{-2} , below which no coastal sea defences are built, as these regions are considered (nearly) uninhabited⁸⁷.

Supplementary Discussion

Model limitations

We should emphasize that the model presented here is designed to predict the impacts of SLR on coastal wetland development, but does not account for changes in coastal wetland area due to anthropogenic conversion (i.e. land use change). With respect to socio-economic drivers we only consider the limitation of accommodation space, triggered by a (growing) coastal population (e.g. due to more coastal infrastructure). In the past, however, coastal wetland loss has widely been attributed to the conversion of coastal wetlands for agricultural, touristic and residential purposes^{18,100}.

While accounting for dynamic changes in SLR and coastal population, we assume other model parameters, such as tidal range, coastal topography or sediment availability to remain constant throughout the simulation period. Locally, temporal variability in these parameters may result in significantly different responses to what is suggested by our model. Furthermore, our sediment availability term is derived from long-term satellite data, delivering a pixel-specific long-term average with a horizontal resolution of $1/24^\circ$. These data cannot resolve local sediment dynamics on tidal mudflats, which may, however, significantly contribute to the overall sediment supply of a coastal wetland¹⁰¹. Furthermore, tidal mudflats in front of the vegetated tidal wetlands may also accrete sediment and grow vertically in time, hence allowing coastal wetlands to expand seawards. This process has been shown to be linked to the prevailing hydrodynamic conditions¹⁰²⁻¹⁰⁴, but is not included in the presented model due to a lack of appropriate global-scale hydrodynamic data.

Being reliant on data that is available on a global scale, the processes represented within this model are strongly generalized and schematized, implying that locally and regionally, the morphological development of coastal wetlands may significantly deviate from the proposed model^{59,102}. A lack of global data for the vertical evolution of coastal wetlands has also been highlighted by Webb et al.¹⁰⁵ who show that the available data is strongly biased towards North America, Europe and south-eastern Australia.

With respect to the calculation of the inland migration of coastal wetlands, we present a novel approach, whereby migration is calculated based on a schematization of a coastal profile, derived from SRTM data⁴⁷. Conversion of dry upland areas to coastal wetlands is estimated using a bathtub style inundation model, which may overestimate the inundated areas as it does not take into account flow reduction due to surface roughness effects. The employed SRTM data have a vertical resolution of only 1 m, which makes it necessary to linearly interpolate between the different elevation increments. This method has previously been shown to allow for reliable impact modelling for SLR scenarios between 20 cm and 1 m (i.e. our scenarios are well within this range) despite the coarse vertical resolution of the SRTM data^{51,52}. An attempt to quantify the error introduced by linear interpolation of elevation contours along the US east coast revealed a mean error of less than 30 cm and found that the interpolated elevation model was “as likely to overstate as understate the amount of land below a particular elevation”⁵². This independent finding shows the general suitability of linear interpolation for inundation modelling and delivers an estimate for the potential vertical error introduced by this methodology. However, locally, the coastal profile may significantly deviate from the assumption of a linear slope, thus influencing the inundation patterns. Moreover, in our approach we assume lower elevations to be located closer to the sea. This assumption has also been found to generally be representative of global coastal topography³³, but may locally lead

to overestimation of wetland inland migration, if areas of low elevations (that are not hydrologically connected to the sea) are located further inland than higher elevations along the coast.

Additionally, inland migration of coastal wetlands or their ability to vertically adapt to global SLR may locally be affected by tectonic/neotectonic uplift or subsidence, respectively, as tectonic/neotectonic processes other than GIA are not considered in our model. However, on a global scale, we do not expect these processes to significantly affect the modelled wetland extents, as these processes uplift the coast in some regions, whilst lowering it in others. In contrast, human-induced subsidence in some of the large deltas of the world⁶³ exclusively trigger subsidence. This always increases RSLR and may locally reduce the ability of coastal wetland to vertically accrete with SLR. Wetland-internal variability in biophysical and biogeochemical processes (e.g. autocompaction¹⁰⁶, organic decomposition¹⁰⁷, internal waterlogging and vegetation die-off¹⁰⁸) affecting the vertical performance of a coastal wetlands may also introduce a deviation of the assumed overall inland migration of a particular coastal wetland in response to global sea level rise.

References

- 92 Pickering, M. *The impact of future sea-level rise on the tides* (University of Southampton, (2014).
- 93 Lyard, F., Lefevre, F., Letellier, T. & Francis, O. Modelling the global ocean tides: modern insights from FES2004. *Ocean Dynamics* **56**, 394-415 (2006).
- 94 Boumans, R. M. J. & Day, J. W. High precision measurements of sediment elevation in shallow coastal areas using a sedimentation-erosion table. *Estuaries* **16**, 375-380 (1993).
- 95 Cahoon, D. R., Reed, D. J. & Day, J. W. Estimating shallow subsidence in microtidal salt marshes of the southeastern United States: Kaye and Barghoorn revisited. *Marine Geology* **128**, 1-9 (1995).
- 96 Carol, E., Kruse, E. & Tejada, M. Surface water and groundwater response to the tide in coastal wetlands: Assessment of a marsh in the outer Río de la Plata estuary, Argentina. *Journal of Coastal Research* **SI65**, 1098-1103 (2013).
- 97 United Nations. *World Economic Situation and Prospects 2014*. (United Nations, 2014).
- 98 OECD. *Gross national income (indicator)*, Available online: <https://data.oecd.org> (2017).
- 99 OECD. *Gross domestic product (indicator)*, Available online: <https://data.oecd.org> (2017).
- 100 Marcoe, K. & Pilson, S.. Habitat change in the lower Columbia River Estuary, 1870-2009. *Journal of Coastal Conservation* **21**, 505-525 (2017).
- 101 Schuerch, M., Dolch, T., Reise, K. & Vafeidis, A. T. Unravelling interactions between salt marsh evolution and sedimentary processes in the Wadden Sea (southeastern North Sea). *Progress in Physical Geography* **38**, 691-715 (2014).
- 102 Balke, T., Herman, P. M. J. & Bouma, T. J. Critical transitions in disturbance-driven ecosystems: identifying Windows of Opportunity for recovery. *Journal of Ecology* **102**, 700-708 (2014).
- 103 Silinski, A., Fransen, E., Bouma, T. J., Meire, P. & Temmerman, S. Unravelling the controls of lateral expansion and elevation change of pioneer tidal marshes. *Geomorphology* **274**, 106-115 (2016).
- 104 Zhu, Z., Zhang, L., Wang, N., Schwarz, C. & Ysebaert, T. Interactions between the range expansion of saltmarsh vegetation and hydrodynamic regimes in the Yangtze Estuary, China. *Estuarine, Coastal and Shelf Science* **96**, 273-279 (2012).
- 105 Webb, E. L. *et al.* A global standard for monitoring coastal wetland vulnerability to accelerated sea-level rise. *Nature Climate Change* **3**, 458-465 (2013).
- 106 Allen, J. R. L. Morphodynamics of Holocene salt marshes: a review sketch from the Atlantic and Southern North Sea coasts of Europe. *Quaternary Science Reviews* **19**, 1155-1231 (2000).
- 107 Kirwan, M., Langley, J., Guntenspergen, G. R. & Magonigal, J. The impact of sea-level rise on organic matter decay rates in Chesapeake Bay brackish tidal marshes. *Biogeosciences* **10**, 1869-1876 (2013).
- 108 Alber, M., Swenson, E. M., Adamowicz, S. C. & Mendelsohn, I. A. Salt Marsh Dieback: An overview of recent events in the US. *Estuarine, Coastal and Shelf Science* **80**, 1-11 (2008).